Eur. Phys. J. C 52, 339–355 (2007)
DOI 10.1140/epjc/s10052-007-0395-3

THE EUROPEAN PHYSICAL JOURNAL C

Regular Article – Theoretical Physics

Two-photon exchange contributions to elastic ep scattering in the non-local field formalism

P. Jain[a], S.D. Joglekar[b], S. Mitra[c]

Department of Physics, IIT Kanpur, Kanpur, 208016, India

Received: 7 September 2006 / Revised version: 12 July 2007 /
Published online: 6 September 2007 –

Abstract. We construct a non-local gauge-invariant Lagrangian to model the electromagnetic interaction of the proton. The Lagrangian includes all allowed operators with dimension up to five. We compute the two-photon exchange contribution to elastic electron–proton scattering using this effective non-local Lagrangian. The one-loop calculation in this model includes the standard box and cross box diagram with the standard on-shell form of the hadron electromagnetic vertices. Besides this we find an extra contribution, which depends on an unknown constant. We use experimentally extracted form factors for our calculation. We find that the correction to the reduced cross section is slightly non-linear as a function of the photon longitudinal polarization ε. The non-linearity seen is within the experimental error bars of the Rosenbluth data. The final result completely explains the difference between the form factor ratio $G_{\rm E}/G_{\rm M}$ extracted by Rosenbluth separation technique at SLAC and polarization transfer technique at JLAB.

1 Introduction

The electromagnetic form factors F_1 and F_2 parametrize the vertex of the electromagnetic interaction of a photon with an on-shell proton,

$$\Gamma_\mu(p,p') = \gamma_\mu F_1(q^2) + \frac{\mathrm{i}\kappa_p}{2M_p} F_2(q^2)\sigma_{\mu\nu}q^\nu\,, \qquad (1)$$

where p and p' are the initial and final proton momenta, M_p is the proton mass, κ_p its anomalous magnetic moment and $q = p' - p$ is the momentum transfer. The functions F_1 and F_2 are called the Dirac and Pauli form factors respectively. They are experimentally measured by elastic scattering of electrons on protons, assuming that the process is dominated by one-photon exchange diagram (Fig. 1). We also define $Q^2 = -q^2 \geq 0$. Besides the form factors F_1 and F_2, it is also convenient to define the electric and magnetic form factors (or the Sachs form factors), $G_{\rm E}$ and $G_{\rm M}$, which are more suitable for experimental extraction:

$$\begin{aligned} G_{\rm E}(Q^2) &= F_1(Q^2) - \tau\kappa_p F_2(Q^2)\,,\\ G_{\rm M}(Q^2) &= F_1(Q^2) + \kappa_p F_2(Q^2)\,, \end{aligned} \qquad (2)$$

where $\tau = Q^2/4M_p^2$. At $Q^2 = 0$, $F_1 = F_2 = 1$ and $G_{\rm E} = G_{\rm M}/\mu_p = 1$, where μ_p is the magnetic moment of the proton. The form factor $G_{\rm M} \approx \mu_p G_{\rm D}$ where $G_{\rm D}$ is the dipole function,

$$G_{\rm D} = \frac{1}{\left(1 + \frac{Q^2}{0.71}\right)^2}\,. \qquad (3)$$

At low momenta, $G_{\rm E}$ is also approximately equal to $G_{\rm D}$. At large momenta, $Q^2 \gg 1\ \mathrm{GeV}^2$,

$$G_{\rm M}, F_1 \propto \frac{1}{Q^4}\,. \qquad (4)$$

The experimental status of $G_{\rm E}$ and F_2 is, however, currently unclear at large momentum transfer.

A standard technique for the extraction of the proton form factors is the Rosenbluth separation [1]. Here one considers the unpolarized elastic scattering of electrons on target protons. In the one-photon exchange approximation the cross section can be written as

$$\frac{\mathrm{d}\sigma}{\mathrm{d}\Omega} = \frac{\sigma_{\rm Mott}}{\varepsilon(1+\tau)}\left[\tau G_{\rm M}^2(Q^2) + \varepsilon G_{\rm E}^2(Q^2)\right], \qquad (5)$$

where $\varepsilon = 1/[1 + 2(1+\tau)\tan^2(\theta_e/2)]$ is the longitudinal polarization of the photon and θ_e is the electron scattering angle. One finds that the reduced cross section, $\sigma_{\rm R} = \tau G_{\rm M}^2(Q^2) + \varepsilon G_{\rm E}^2(Q^2)$ depends linearly on ε. By making a linear fit to the observed $\sigma_{\rm R}$ as a function ε at fixed Q^2, one can, therefore, extract both $G_{\rm M}$ and $G_{\rm E}$. At large Q^2, $G_{\rm M}$ dominates at all values of ε. Hence the uncertainty in the extraction of $G_{\rm E}$ can be large at large Q^2. Recent results for Rosenbluth separation are available from SLAC [2,3] and JLAB [4]. The SLAC data shows

[a] e-mail: pkjain@iitk.ac.in
[b] e-mail: sdj@iitk.ac.in
[c] e-mail: subha@iitk.ac.in

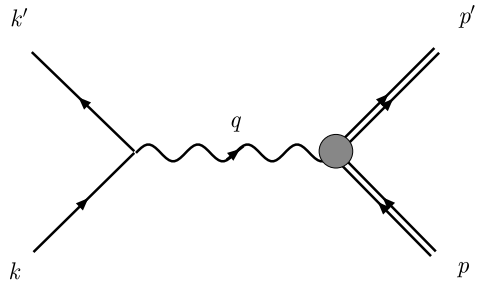

Fig. 1. The one-photon exchange diagram contributing to the elastic electron–proton scattering. Here k and k' refer to the initial and final electron momenta and p and p' to the initial and final proton momenta respectively. $q = k - k' = p' - p$ is the momentum exchanged

that $\frac{\mu_p G_\mathrm{E}}{G_\mathrm{M}} \approx 1$ up to momentum transfer $Q^2 \approx 6\,\mathrm{GeV}^2$. The JLAB data is available at $Q^2 = 2.64, 3.20$ and $4.10\,\mathrm{GeV}^2$ and shows a similar trend. This result also implies that the ratio $F_2/F_1 \propto 1/Q^2$.

A direct extraction of the ratio $G_\mathrm{E}/G_\mathrm{M}$ is possible by elastic scattering of longitudinally polarized electrons on a target proton, $\vec{e} + p \to e + \vec{p}$ [5–10]. In the one-photon exchange approximation, the recoiling proton acquires only two polarization components, P_l, parallel to the proton momentum and P_t, perpendicular to the proton momentum in the scattering plane. The ratio obeys

$$\frac{G_\mathrm{E}}{G_\mathrm{M}} = -\frac{P_\mathrm{t}}{P_\mathrm{l}} \frac{E_e + E'_e}{2M_p} \tan\left(\frac{\theta_e}{2}\right), \tag{6}$$

where E_e and E'_e are the energies of the initial and final electron. This technique, therefore, directly yields the ratio $G_\mathrm{E}/G_\mathrm{M}$. The results [11–14], available from JLAB, show that $\mu_p G_\mathrm{E}/G_\mathrm{M}$ decreases with Q^2. A straight line fit to the data gives

$$\frac{\mu_p G_\mathrm{E}}{G_\mathrm{M}} \approx 1.06 - 0.15 Q^2, \tag{7}$$

in the momentum range $0.5 < Q^2 < 5.6\,\mathrm{GeV}^2$. The ratio, therefore, becomes as small as 0.2 at $Q^2 = 5.6\,\mathrm{GeV}^2$, the maximum momentum transfer in this experiment. The polarization transfer results also imply that $QF_2/F_1 \sim 1$ for $Q^2 > 1\,\mathrm{GeV}^2$. The observed trend in the polarization transfer experiment is, therefore, completely different from what is measured using the Rosenbluth separation. This is clearly a serious problem and has attracted considerable attention in the literature [15, 16].

2 Two-photon exchange

An obvious source of error is the higher order corrections to the elastic scattering process. A reliable extraction of the form factors requires a careful treatment of the radiative corrections including the soft photon emission, which give a significant correction to the cross section [17–20]. These contributions are calculated by keeping only the leading order terms in the soft photon momentum. Furthermore only the infrared divergent terms, which are required to cancel the divergences in the soft photon emission, are included in the radiative corrections. It is possible that the terms not included in these calculations may be responsible for the observed difference. Any such correction is likely to be small and hence cannot significantly change the results of the polarization transfer experiment. However, a small correction to the Rosenbluth separation could imply a large correction to the extracted form factor G_E. A possible correction is the two-photon exchange diagram, which has attracted considerable attention in the literature [21–27]. Such a diagram is taken into account while computing the radiative corrections, but only the infrared divergent contribution is included. It is possible that the remaining contribution gives a significant correction. One may also consider next to leading order corrections in the soft photon momenta to the soft photon emission diagrams. Both of these contributions receive unknown hadronic corrections and cannot be calculated in a model independent manner.

In this paper we estimate the two-photon exchange contribution using an effective non-local Lagrangian. The

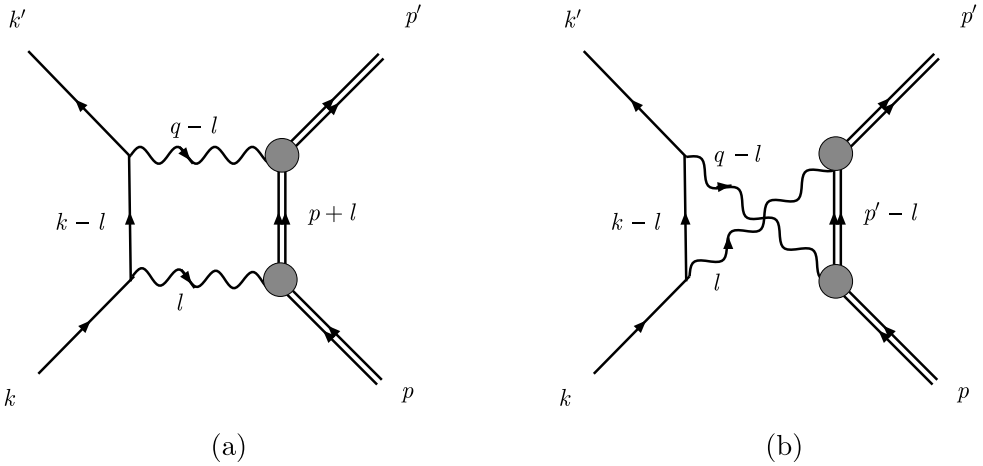

Fig. 2. The two-photon exchange diagrams contributing to the elastic electron–proton scattering: **a** box diagram and **b** cross box diagram

box and cross box diagrams that contribute are shown in Fig. 2a and b respectively. As discussed later, in the non-local formalism we need to evaluate one more diagram. The two-photon contribution has also been obtained by model calculations in [23–25]. The authors find that they are able to partially reconcile the discrepancy. The results of [23–25] show that the predicted Rosenbluth plots are no longer linear in ε. The experimental results obtained from JLAB [4] show very little deviation from linearity. The SLAC results [3] can incorporate some non-linearity due to the presence of relatively larger error bars. The present limit on the deviation from linearity is given in [28]. In [26] the authors argue, using charge conjugation and crossing symmetry, that two-photon exchange contribution must necessarily be non-linear in ε. If the two-photon exchange contribution shows large non-linearity as a function of ε, then it cannot provide an explanation of the observed anomaly.

3 General electromagnetic vertex of proton

The elementary electromagnetic vertex of an on-shell proton is given in (1). When the proton is off-shell, the vertex is expected to be more general. Further, it must satisfy the WT identity, following from gauge invariance, which implies a relation between $\Gamma_\mu(p,p')$ and the inverse proton propagator, $S_{\rm F}^{-1}(p)$. A *local* theory of interaction of a proton and a photon would have a U(1) gauge invariance implied by *local* transformations and would imply the WT identity:

$$q^\mu \Gamma_\mu(p,p') = S_{\rm F}^{-1}(p') - S_{\rm F}^{-1}(p)\,. \tag{8}$$

This identity would be violated if in calculating the two-photon exchange diagrams one uses the standard on-shell form factors defined in (1) and a free proton propagator. Here we are interested in formulating the theory in terms of an effective *non-local* action, which will allow us to maintain gauge invariance in the presence of form factors in the electromagnetic interaction of proton. It is certainly possible to maintain gauge invariance in a local theory also, but in this case the form factors will arise only after we take into account loop corrections in the strong interactions. It is not clear how to systematically do calculations in such a case. In the present case the form factors are present at the tree-level interaction of a photon with a proton. The vertex $\Gamma_\mu(p,p')$ satisfies a generalized *non-local* version of the WT identity:[1]

$$g\left(q^2\right) q^\mu \Gamma_\mu(p,p') = S_{\rm F}^{-1}(p') - S_{\rm F}^{-1}(p)\,, \tag{9}$$

where $g\left(q^2\right)$ is a function of q^2 appearing in the gauge-transformation equations, ultimately to be related to a form factor in the next section. As we shall see in the next section, this identity follows from a non-local electromagnetic invariance and in fact is more appropriate for an extended object like a proton. In the local limit, the function $g(q^2) \to 1$, and the identity in (9) reduces to the local WT identity. On account of the charge-conjugation invariance of the proton–photon interaction, the vertex $\Gamma_\mu(p,p')$, a 4×4 matrix, must satisfy[2]

$$C^{-1}\Gamma_\mu(p,p')C = -\Gamma_\mu^{\rm T}(-p',-p)\,, \tag{10}$$

where C is the charge-conjugate matrix, with $C\gamma_\mu C^{-1} = -\gamma_\mu^{\rm T}$[3] We now express the vertex in its most general form, employing the 16 linearly independent Dirac matrices, 1, γ_5, γ_μ, $\gamma_\mu\gamma_5$ and $\sigma_{\mu\nu}$, and the 4-vectors $P^\mu \equiv (p+p')^\mu$ and $q^\mu \equiv (p'-p)^\mu$. We get

$$\begin{aligned}\Gamma_\mu(p,p') = {} & aP_\mu + bq_\mu + c\gamma_\mu \\ & + d\,\not{P}P_\mu + e\,\not{P}q_\mu + f\,\not{q}P_\mu + g\,\not{q}q_\mu \\ & + h\sigma_{\mu\alpha}P^\alpha + j\sigma_{\mu\alpha}q^\alpha \\ & + k\sigma_{\alpha\beta}P^\alpha q^\beta P_\mu + l\sigma_{\alpha\beta}P^\alpha q^\beta q_\mu \\ & + m\gamma_\alpha\gamma_5\xi_\mu^{\nu\alpha\beta}P_\beta q_\nu\,. \end{aligned} \tag{11}$$

Here, the 12 coefficients $a, b, \ldots, m$ are functions of the three Lorentz invariants p^2, p'^2 and q^2. Charge conjugation requires that a, c, d, g, j and k are *symmetric* under $p^2 \leftrightarrow p'^2$ and b, e, f, h, l and m are antisymmetric under the same operation. To implement the WT identity, we write the expression

$$S_{\rm F}^{-1}(p) = \alpha\left(p^2\right)\not{p} + \beta\left(p^2\right) \tag{12}$$

in its most general form. We then impose the WT identity given in (9). This leads to some constraints between the coefficients. The net result of all this is the following form for Γ_μ:

$$\begin{aligned}\Gamma_\mu(p,p') = {} & a'P_\mu + c'\gamma_\mu + j\sigma_{\mu\alpha}q^\alpha + d'\,\not{P}P_\mu \\ & + 7 \text{ divergence free terms}\,. \end{aligned}$$

We enumerate the divergence free terms (i.e. X_μ with $q^\mu X_\mu \equiv 0$):

$$\begin{aligned} & b'\left[(p'^2-p^2)q_\mu - q^2P_\mu\right] + f\left(-P, q\gamma_\mu + \not{q}P_\mu\right) \\ & + g\left(-q^2\gamma_\mu + \not{q}q_\mu\right) + k\left(-\sigma_{\mu\alpha}P^\alpha P, q + \sigma_{\alpha\beta}P^\alpha q^\beta P_\mu\right) \\ & + l\left(\sigma_{\mu\alpha}P^\alpha q^2 - \sigma_{\beta\alpha}P^\alpha q^\beta q_\mu\right) + e'\left(-q^2\,\not{P}P_\mu + P, q\,\not{P}q_\mu\right) \\ & + m\gamma_\alpha\gamma_5\xi_\mu^{\nu\alpha\beta}P_\beta q_\nu\,. \end{aligned}$$

We further note the relations that arise from the WT identity, and which restrict the *form* of some of the coefficients

[1] Such non-local WT identities generally occur in non-local quantum field theories; see e.g. [29]. This WT identity reduces to the usual one as $q \to 0$, provided $g(0) = 1$.

[2] The negative signs for the momenta on the right-hand side are a consequence of our different sign convention regarding the incoming particle (incoming momentum positive) and the out-going particle (out-going momentum positive).

[3] See e.g. [30].

(a', c') considerably:

$$a' = \frac{\beta\left(p'^2\right) - \beta\left(p^2\right)}{g\left(q^2\right)\left(p'^2 - p^2\right)}\,,$$
$$c' = \frac{\alpha\left(p'^2\right) + \alpha\left(p^2\right)}{2g\left(q^2\right)}\,,$$
$$d' = \frac{\alpha\left(p'^2\right) - \alpha\left(p^2\right)}{g\left(q^2\right)\left(p'^2 - p^2\right)}\,,$$

whereas the coefficients j, b, f, g, k, l and m are completely arbitrary functions of the Lorentz invariants. We make several observations.

1. We note first that power counting would associate all operators except those three with coefficients a', c' and j with a local operator of dimension 6 or higher.
2. We note that the dependence on q^2 of *both* a' and c' are *identical*. Near mass-shell,[4] $\alpha\left(p^2\right) \sim \alpha_0 + \alpha_1[p^2 - M_p^2]$ and $\beta\left(p^2\right) \sim \beta_0 + \beta_1[p^2 - M_p^2]$; and thus,

$$a' = \left\{\beta_1 + \mathcal{O}\left[p^2 - M_p^2\right]\right\} g^{-1}\left(q^2\right)\,,$$
$$c' = \left\{\alpha_0 + \frac{1}{2}\alpha_1\left[p^2 + p'^2 - 2M_p^2\right]\right\} g^{-1}\left(q^2\right)\,. \tag{13}$$

3. The on-shell expression (1) for $\Gamma_\mu(p, p')$ takes operators of dimensions 4 (electric) and 5 (magnetic) into account. It is then logical that the *only* other operator of dimension 5 should also be included in the *off-shell* expression for the $\Gamma_\mu(p, p')$. We shall take these three terms into account in our minimal effective Lagrangian model.

4 Effective Lagrangian model

We represent the interaction of the photon–proton system by an effective non-local Lagrangian model based on the discussion in the previous section. We adopt the following guidelines in the process.

– The Lagrangian model should incorporate up to dimension 5 operators, for reasons partly explained in the previous section. The assumption is that in the effective Lagrangian approach, the higher dimension operators will contribute much less. This is borne out in the calculations performed. (See Fig. 12 and the subsequent discussion.)
– The model should incorporate the results regarding the form of the coefficients a' and c' obtained earlier (see (13)); thus, at least one should embody the form factors on mass-shell. The resulting model is necessarily non-local.
– We assume that the model has lowest order derivatives for the fermions. Our assumption about the dimensionality of the operators is consistent with this.
– We require that this *non-local* model has an equivalent form of gauge invariance. Such constructions of *non-local* versions of local symmetries are known in the literature [29, 31] and we shall show explicitly that our model below has a very simple form of non-local gauge invariance.

A Lagrangian model that satisfies these constraints is given by

$$\mathcal{L} = \overline{\psi}\left(\mathrm{i}\,\partial\!\!\!/ - e f_1'\left[\frac{\partial^2}{\Lambda^2}\right] A\!\!\!/ - M_p\right)\psi + \frac{a''}{2M_p}\overline{\psi}\left(\sigma_{\mu\nu} f_2'\left[\frac{\partial^2}{\Lambda^2}\right] F^{\mu\nu}\right)\psi + \frac{b''}{2M_p}\overline{\psi}\widetilde{D}^2\psi,$$

where $\mathrm{i}\widetilde{D} = \mathrm{i}\partial - e f_1'\left[\frac{\partial^2}{\Lambda^2}\right] A$ is the *non-local covariant* derivative. We point out that the form factors, f_1' and f_2', are to be extracted directly from experiments. We make a number of observations regarding this effective Lagrangian.

1. $\mathcal{L}$ is invariant under the *non-local* form of gauge transformations:

$$\delta A_\mu = -\partial_\mu \alpha\left(x\right);$$
$$\psi(x) \to \mathrm{e}^{\mathrm{i}e f_1'\left[\frac{\partial^2}{\Lambda^2}\right]\alpha(x)}\psi(x)\,,$$
$$\overline{\psi}(x) \to \overline{\psi}(x)\,\mathrm{e}^{-\mathrm{i}e f_1'\left[\frac{\partial^2}{\Lambda^2}\right]\alpha(x)}$$

or equivalently,

$$\delta A_\mu = -\partial_\mu f_1'^{-1}\left[\frac{\partial^2}{\Lambda^2}\right]\beta\left(x\right)\,,$$
$$\psi(x) \to \mathrm{e}^{\mathrm{i}e\beta(x)}\psi(x)\,,$$
$$\overline{\psi}(x) \to \overline{\psi}(x)\,\mathrm{e}^{-\mathrm{i}e\beta(x)}\,.$$

In the latter form, the gauge transformations are similar to the usual local ones, with the exception that in the first of these $\partial_\mu \to \partial_\mu f_1'^{-1}\left(\frac{\partial^2}{\Lambda^2}\right)$. This leads to the non-local WT identity of (9); i.e., one with a replacement $q_\mu \to q_\mu f_1'^{-1}\left(\frac{-q^2}{\Lambda^2}\right) \equiv q_\mu g(q^2)$ in (8). Under this transformation, $F^{\mu\nu}$ and hence the second term is gauge invariant, independent of the form of f_2'. Also, the non-local gauge-covariant derivative satisfies $\widetilde{D}\psi \to \mathrm{e}^{\mathrm{i}e\beta(x)}\widetilde{D}\psi(x)$.
2. The last term generates a term proportional to P_μ in $\Gamma_\mu(p, p')$ with a form factor proportional to f_1', the *same one* appearing in the electric term. This is consistent with the comment on the form of a' and c' given earlier.
3. The (non-local) gauge invariance of the last term requires that it is composed of the (non-local) gauge-covariant derivative: this restricts the form factor present in this term as above.
4. The Lagrangian is exactly valid as long as the proton is on-shell, irrespective of the value of the momentum transfer q^2. In this limit the interaction of the proton with the photon is described in terms of the

[4] The condition that $S_{\mathrm{F}}(p) \sim \frac{1}{\not{p} - M_p}$ near mass-shell requires that $\alpha_0 M_p + \beta_0 = 0$ and $\alpha_0 + 2M_p^2\alpha_1 + 2M_p\beta_1 = 1$.

two form factors and no higher dimensional terms are required. The higher derivative terms we drop give higher order contributions in powers of $(P^2 - M_p^2)/\Lambda^2$, where $P^2 - M_p^2$ is the off-shellness of the proton momentum. These higher order terms can be dropped as long as the dominant contribution to a process is obtained from the kinematic region where $(P^2 - M_p^2)/\Lambda^2 \ll 1$.

5. In the limit $\Lambda \to \infty$ we reproduce the local field theory model for a proton with an anomalous magnetic moment.

Before we proceed, a comment on the non-local form of gauge invariance is in order. It appears that *a local* form of gauge invariance for *extended* particles such as a proton is inappropriate. Consider the wave-function of an extended particle centered at $\mathbf{x}$, viz. $\psi(\mathbf{x}, t)$. Let $\mathbf{y}$ be a point within the charge radius R of the proton: $|\mathbf{x} - \mathbf{y}| < R$. Let us imagine that a gauge transformation on A_μ is carried out (at t) around $\mathbf{y}$ with a very narrow support, ρ: $\rho \ll |\mathbf{x} - \mathbf{y}|$. In the model of fundamental constituents, the quark wave-function should be affected around $\mathbf{y}$, which in turn should affect the proton wave-function *even though* the gauge transformation at $\mathbf{x}$, depending on $\alpha(x)$, will be zero. Thus, the proton wave-function should be affected by a local gauge transformation with a support anywhere in its charge radius. The above form of non-local version of gauge transformations embodies this idea. Note that the Fourier transform of $f_1'\left[\frac{\partial^2}{\Lambda^2}\right]$ has a support over a distance $\sim 1/\Lambda \sim R$.

It proves convenient to rearrange the Lagrangian as follows[5] (recall the relation $\not{D}^2 = D^2 + \frac{e}{2}\sigma_{\mu\nu}F^{\mu\nu}$):

$$\mathcal{L} = \overline{\psi}\left(\mathrm{i}\,\widetilde{\not{D}} - M_p\right)\psi + \frac{\tilde{a}}{2M_p}\overline{\psi}\left(\sigma_{\mu\nu}f_2'\left[\frac{\partial^2}{\Lambda^2}\right]F^{\mu\nu}\right)\psi + \frac{\bar{b}}{2M_p}\overline{\psi}\left(i\,\widetilde{\not{D}} - M_p\right)^2\psi\,.$$

Had there been no magnetic term, the last term would have formally vanished by the classical equation of motion. We note that inclusion of the last term has now modified the inverse propagator: it has non-vanishing terms at $e = 0$. This, in particular, gives a spurious pole in the propagator at another value of $\not{p}$. This problem can be avoided if we can write the $\mathcal{L}$ in the following form:

$$\mathcal{L} = \overline{\psi}\left(\mathrm{i}\,\widetilde{\not{D}} - M_p\right)\exp\left\{\frac{\bar{b}}{2M_p}\left(\mathrm{i}\,\widetilde{\not{D}} - M_p\right)\right\}\psi + \frac{\bar{a}}{2M_p}\overline{\psi}\left(\sigma_{\mu\nu}f_2'\left[\frac{\partial^2}{\Lambda^2}\right]F^{\mu\nu}\right)\psi\,, \tag{14}$$

which is now understood to have been consistently truncated to a given order in $\bar{b}$. We now note that the inverse propagator is

$$(\not{p} - M_p)\exp\left\{\frac{\bar{b}}{2M_p}(\not{p} - M_p)\right\}$$

and has only one zero at $\not{p} - M_p = 0$, and the residue of the propagator at the pole is 1. (In this form of $\mathcal{L}$, $\bar{a}$ is related to the anomalous magnetic moment, κ_p, by the relation $\bar{a} = e\kappa_p/2$, and M_p is the physical mass). Since we shall consider, in the two-photon exchange calculation, terms with the last operator of dimension 5 inserted in *two* photon vertices, we shall do the entire calculation consistently to $\mathcal{O}\left(\bar{b}^2\right)$ using (14). In this case, the propagator for the proton is

$$\frac{\mathrm{i}}{\not{p} - M_p}\exp\left\{-\frac{\bar{b}}{2M_p}(\not{p} - M_p)\right\} \approx \frac{\mathrm{i}}{\not{p} - M_p} - \frac{\mathrm{i}\bar{b}}{2M_p} + \frac{\mathrm{i}\bar{b}^2}{8M_p^2}(\not{p} - M_p)\,.$$

5 Reduction of the action

In this section, we shall find an effective way to calculate the matrix elements involving insertion of the last term in the action. Since a two-photon exchange diagram at one loop is at most $\mathcal{O}[\bar{b}^2]$, we shall evaluate the effect of this term to $\mathcal{O}[\bar{b}^2]$. What we are interested in are the *tree* order matrix elements of two (possibly virtual) photon emission from an *on-shell* proton. The calculation of these can be simplified considerably *in this context* with the use of the fermion equations of motion. The result is simple: of all the terms up to $\mathcal{O}[\bar{b}^2]$, viz. $\mathcal{O}[\bar{b}, \bar{b}\bar{a}, \bar{b}^2, \bar{b}^2\bar{a}, \bar{b}^2\bar{a}^2]$, only the last term of $\mathcal{O}[\bar{b}^2\bar{a}^2]$ gives a non-zero result. While the result can be worked out, it is most effectively dealt with in the path-integral formulation.

We define

$$W[J^\mu, K, \overline{K}] = \int D\phi \exp\left\{\mathrm{i}\int \mathrm{d}^4x \times \left(\mathcal{L} + J^\mu A_\mu + \overline{K}\psi + \overline{\psi}K\right)\right\},$$

where $\mathcal{L}$ is the action of (14) and $D\phi$ denotes generically the measure of the path integral. We now perform a field transformation:

$$\psi = \exp\left\{-\frac{\bar{b}}{2M_p}\left(\mathrm{i}\,\widetilde{\not{D}} - M_p\right)\right\}\psi'. \tag{15}$$

Under this transformation, the Jacobian is

$$J = \det\exp\left\{-\frac{\bar{b}}{2M_p}\left(\mathrm{i}\,\widetilde{\not{D}} - M_p\right)\right\} = \exp\mathrm{tr}\left\{-\frac{\bar{b}}{2M_p}\left(\mathrm{i}\,\widetilde{\not{D}} - M_p\right)\right\} = \exp\mathrm{tr}\left\{\frac{\bar{b}}{2}\mathcal{I}\right\} = \text{a constant}\,, \tag{16}$$

[5] Actually, the constant M_p and the normalization of the KE term are also modified below. However, we shall soon modify the form of the Lagrangian further, where this proves unnecessary.

and hence it can be ignored for the connected Green's functions. This then yields

$$
\begin{aligned}
&W\left[J^\mu, K, \overline{K}\right] \\
&= \int D\phi \exp\left\{ \mathrm{i} \int \mathrm{d}^4x \left[\overline{\psi} \left(\mathrm{i}\widetilde{\not{D}} - M_p \right) \psi' \right.\right. \\
&\quad + \frac{\bar{a}}{2M_p} \overline{\psi} \left(\sigma_{\mu\nu} f_2' \left[\frac{\partial^2}{\Lambda^2} \right] F^{\mu\nu} \right) \\
&\quad \times \exp\left\{ -\frac{\bar{b}}{2M_p} \left(\mathrm{i}\widetilde{\not{D}} - M_p \right) \right\} \psi' \Big] \Big\} \\
&\quad \times \exp \mathrm{i} \left\{ \int \mathrm{d}^4x \Big[J^\mu A_\mu + \overline{\psi} K \right. \\
&\quad \left.\left. + \overline{K} \exp\left\{ -\frac{\bar{b}}{2M_p} \left(\mathrm{i}\widetilde{\not{D}} - M_p \right) \right\} \psi' \Big] \right\}.
\end{aligned}
$$

We note that if we had $\bar{a} = 0$, we would have no left-over term in the *action*. It is easy to show that $\overline{K} \left[\exp\left\{ -\frac{\bar{b}}{2M_p} \left[\mathrm{i}\widetilde{\not{D}} - M_p \right] \right\} - 1 \right] \psi'$ does not contribute to *tree-level on-shell* proton matrix elements.[6] Thus all tree-level on-shell two-proton matrix elements involving the last term in (14) are at least of order $\bar{a}\bar{b}$. We now expand the action to $\mathcal{O}[\bar{b}^2]$. We find

$$
\begin{aligned}
&W[J^\mu, K, \overline{K}] \\
&= \int D\phi \exp\left\{ \mathrm{i} \int \mathrm{d}^4x \left[\mathcal{L}' + J^\mu A_\mu + \overline{K}\psi' + \overline{\psi} K \right] \right\} \\
&\quad + \mathcal{O}[\bar{b}^3] \,,
\end{aligned}
$$

with

$$
\begin{aligned}
\mathcal{L}' = &\left[\overline{\psi} + \frac{\bar{a}}{2M_p} \overline{\psi} \left(\sigma_{\mu\nu} f_2' \left[\frac{\partial^2}{\Lambda^2} \right] F^{\mu\nu} \right) \right. \\
&\left. \times \left\{ -\frac{\bar{b}}{2M_p} + \frac{\bar{b}^2}{8M_p^2} \left(\mathrm{i}\widetilde{\not{D}} - M_p \right) \right\} \right] \left(\mathrm{i}\widetilde{\not{D}} - M_p \right) \psi' \\
&+ \frac{\bar{a}}{2M_p} \overline{\psi} \left(\sigma_{\mu\nu} f_2' \left[\frac{\partial^2}{\Lambda^2} \right] F^{\mu\nu} \right) \psi' \,.
\end{aligned}
$$

We now perform another field transformation:

$$
\begin{aligned}
&\overline{\psi} + \frac{\bar{a}}{2M_p} \overline{\psi} \left(\sigma_{\mu\nu} f_2' \left[\frac{\partial^2}{\Lambda^2} \right] F^{\mu\nu} \right) \\
&\times \left\{ -\frac{\bar{b}}{2M_p} + \frac{\bar{b}^2}{8M_p^2} \left(\mathrm{i}\widetilde{\not{D}} - M_p \right) \right\} \\
&= \overline{\psi}' \equiv \overline{\psi}[1 + X] \,. \qquad (17)
\end{aligned}
$$

We can write

$$
\begin{aligned}
\overline{\psi} = \overline{\psi}' &\left[1 + \frac{\bar{a}}{2M_p} \left(\sigma_{\mu\nu} f_2' \left[\frac{\partial^2}{\Lambda^2} \right] F^{\mu\nu} \right) \right. \\
&\left. \times \left\{ -\frac{\bar{b}}{2M_p} + \frac{\bar{b}^2}{8M_p^2} \left(\mathrm{i}\widetilde{\not{D}} - M_p \right) \right\} \right]^{-1}
\end{aligned}
$$

$$
\begin{aligned}
&= \overline{\psi}' + \overline{\psi}' \left(-\frac{\bar{a}}{2M_p} \right) \left(\sigma_{\mu\nu} f_2' \left[\frac{\partial^2}{\Lambda^2} \right] F^{\mu\nu} \right) \\
&\quad \times \left\{ -\frac{\bar{b}}{2M_p} + \frac{\bar{b}^2}{8M_p^2} \left(\mathrm{i}\widetilde{\not{D}} - M_p \right) \right\} \\
&\quad + \mathcal{O}\left[F^2\right] .
\end{aligned}
$$

Terms $\mathcal{O}[F^2]$ will not matter for the present calculation of two-photon exchange, as it will give a term having three photon fields. The Jacobian for this transformation is

$$
\begin{aligned}
1/J' &= \det[1 + X] = \det\left[1 + X + \frac{X^2}{2} - \frac{X^2}{2} + \mathcal{O}\left[\bar{b}^3\right] \right] \\
&= \det\left[\mathrm{e}^X - \frac{X^2}{2} + \mathcal{O}\left[\bar{b}^3\right] \right] \\
&= \det \mathrm{e}^X \det\left[1 - \mathrm{e}^{-X} \frac{X^2}{2} + \mathcal{O}\left[\bar{b}^3\right] \right] \\
&= \exp[\mathrm{tr} X] \det\left[1 - \mathrm{e}^{-X} \frac{X^2}{2} \right] \\
&= 1 - \mathrm{tr}\left(\mathrm{e}^{-X} \frac{X^2}{2} \right) + \mathcal{O}\left[\bar{b}^3\right] \\
&= 1 - \mathrm{tr} \frac{X^2}{2} + \mathcal{O}\left[\bar{b}^3\right] \\
&= 1 - \frac{\bar{a}^2 \bar{b}^2}{32 M_p^4} f_2' \left[\frac{\partial^2}{\Lambda^2} \right] F_{\mu\nu} f_2' \left[\frac{\partial^2}{\Lambda^2} \right] F^{\mu\nu} \times (\text{constant}) \,.
\end{aligned}
$$

The last term does not contribute to the emission of two photons from a proton line in the tree approximation. As a result of the transformation (17), the action then becomes

$$
\begin{aligned}
\mathcal{L}'' = &\overline{\psi}' \left(\mathrm{i}\widetilde{\not{D}} - M_p \right) \psi' + \frac{\bar{a}}{2M_p} \overline{\psi}' \left(\sigma_{\mu\nu} f_2' \left[\frac{\partial^2}{\Lambda^2} \right] F^{\mu\nu} \right) \psi' \\
&+ \left(\frac{\bar{a}}{2M_p} \right)^2 \left(\frac{\bar{b}}{2M_p} \right) \overline{\psi}' \left(\sigma_{\mu\nu} f_2' \left[\frac{\partial^2}{\Lambda^2} \right] F^{\mu\nu} \right)^2 \psi' \\
&- \left(\frac{\bar{a}}{2M_p} \right)^2 \left(\frac{\bar{b}^2}{8M_p^2} \right) \overline{\psi}' \left(\sigma_{\alpha\beta} f_2' \left[\frac{\partial^2}{\Lambda^2} \right] F^{\alpha\beta} \right) \\
&\times \left(\mathrm{i}\widetilde{\not{D}} - M_p \right) \left(\sigma_{\mu\nu} f_2' \left[\frac{\partial^2}{\Lambda^2} \right] F^{\mu\nu} \right) \psi' + \mathcal{O}[\bar{b}^3]
\end{aligned}
$$

and the source term transforms into

$$
\begin{aligned}
&\overline{\psi}'[1 + X]^{-1} K \\
&= \overline{\psi}' \left[1 + \left(-\frac{\bar{a}}{2M_p} \right) \left(\sigma_{\mu\nu} f_2' \left[\frac{\partial^2}{\Lambda^2} \right] F^{\mu\nu} \right) \right. \\
&\quad \left. \times \left\{ -\frac{\bar{b}}{2M_p} + \frac{\bar{b}^2}{8M_p^2} \left(\mathrm{i}\widetilde{\not{D}} - M_p \right) \right\} \right] K \\
&\quad + \overline{\psi}' \left(\frac{\bar{a}}{2M_p} \right) \left(\frac{\bar{b}^2}{8M_p^2} \right) \left(\sigma_{\alpha\beta} f_2' \left[\frac{\partial^2}{\Lambda^2} \right] F^{\alpha\beta} \right) \\
&\quad \times \left(\sigma_{\mu\nu} f_2' \left[\frac{\partial^2}{\Lambda^2} \right] F^{\mu\nu} \right) K \,.
\end{aligned}
$$

None of these terms contributes to the tree approximation two-photon matrix element for reasons similar as before.

In conclusion, when we look at the two-photon exchange diagrams having up to two insertions of the last

[6] This is because one does not have a pole in at least one of the external momenta; it is forbidden either by an explicit factor of $\not{p} - M_p$ or by a vertex.

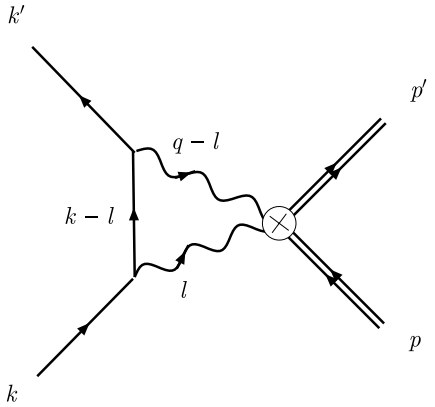

Fig. 3. The two-photon exchange diagram proportional to $\bar{b}^2$ contributing to the elastic electron–proton scattering. The Feynman rule for this diagram can be obtained from (18)

term in (14), each set of diagrams contains a common part, viz., two- (unphysical) photon tree amplitude from an on-shell proton. The above discussion shows that the net effect of that comes from the terms

$$\left(\frac{\bar{a}}{2M_p}\right)^2\left(\frac{\bar{b}}{2M_p}\right)\overline{\psi}'\left(\sigma_{\mu\nu}f_2'\left[\frac{\partial^2}{\Lambda^2}\right]F^{\mu\nu}\right)^2\psi' - \left(\frac{\bar{a}}{2M_p}\right)^2\left(\frac{\bar{b}^2}{8M_p^2}\right)\overline{\psi}'\left(\sigma_{\alpha\beta}f_2'\left[\frac{\partial^2}{\Lambda^2}\right]F^{\alpha\beta}\right)\left(\mathrm{i}\,\widetilde{\not{D}} - M_p\right) \times\left(\sigma_{\mu\nu}f_2'\left[\frac{\partial^2}{\Lambda^2}\right]F^{\mu\nu}\right)\psi'\,. \quad (18)$$

We shall show in Appendix A that the first term does not contribute in the Feynman gauge. That leaves us with only the last term. The Feynman diagram corresponding to this term is shown in Fig. 3.

6 Calculation and results

In this section we give details of the calculation of the two-photon exchange diagrams using our effective Lagrangian. The calculation turns out to be complicated due to the explicit presence of form factors at the vertices. We also require models for the form factors both in the space-like and time-like regions. In the space-like region the form factor $F_1(q^2)$ is known reasonably well. In the time-like region experimental data exist for the form factor $G_{\mathrm{M}}(q^2)$ for $4M_p^2 < q^2 < 14\,\mathrm{GeV}^2$, where $4M_p^2$ is the threshold energy for $p\bar{p}$ production. In [32], $G_{\mathrm{M}}(q^2)$ has been extracted in the unphysical region $0 < q^2 < 4M_p^2$ by using dispersion relations [33, 34]. The extracted form factor shows two resonances at masses $M \sim 770\,\mathrm{MeV}$ and $M \sim 1600\,\mathrm{MeV}$. The phase of the magnetic form factor also shows a large variation in the unphysical region. The electric form factor $G_{\mathrm{E}}(q^2)$, however, is not well known. The amplitude in the unphysical region is obtained in [35]. However, the phase is not known. The form factors G_{E} and G_{M} in the unphysical region can also be extracted using the results given in [34]. The resulting behavior is very different from that obtained in [32]. Such differences may introduce uncertainty in our evaluation of the two-photon exchange contribution, which can hopefully be reduced in future when the form factors are known more accurately. In our evaluation we use the form factors extracted by Baldini et al. [32].

Our model for the form factors is given in Appendix B. We use two different models. Both consist of a sum of simple poles. The corresponding masses and widths are given in Tables 3 and 4. The values of these parameters are obtained by fits to the experimental data or the data obtained from experiments by using dispersion relations [32]. The resulting amplitude and phase of the form factors for the two models are shown in Figs. 4 and 5, respectively.

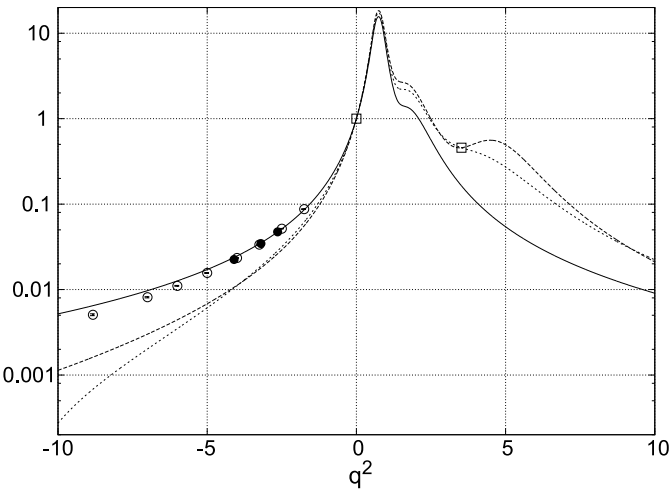

Fig. 4. The amplitude of G_{M}/μ_p (*solid line*) and G_{E} (*dotted line* is for Model I, *dashed line* for Model II). The *unfilled squares* represent the constrained values for G_{E} at $q^2 = 0$ and $q^2 = 4M^2$. Results of Rosenbluth extraction experiments (*filled circles* are for JLAB, *unfilled circles* for SLAC) are also shown

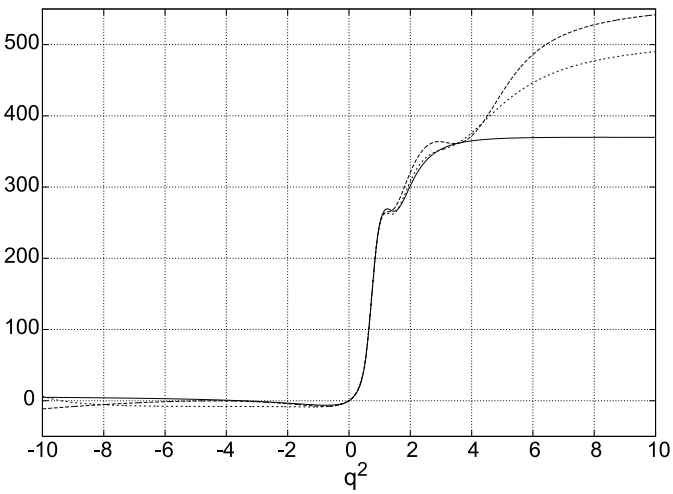

Fig. 5. The phase (in degrees) of G_{M} (*solid line*) and G_{E} (*dotted line* is for Model I, *dashed line* for Model II)

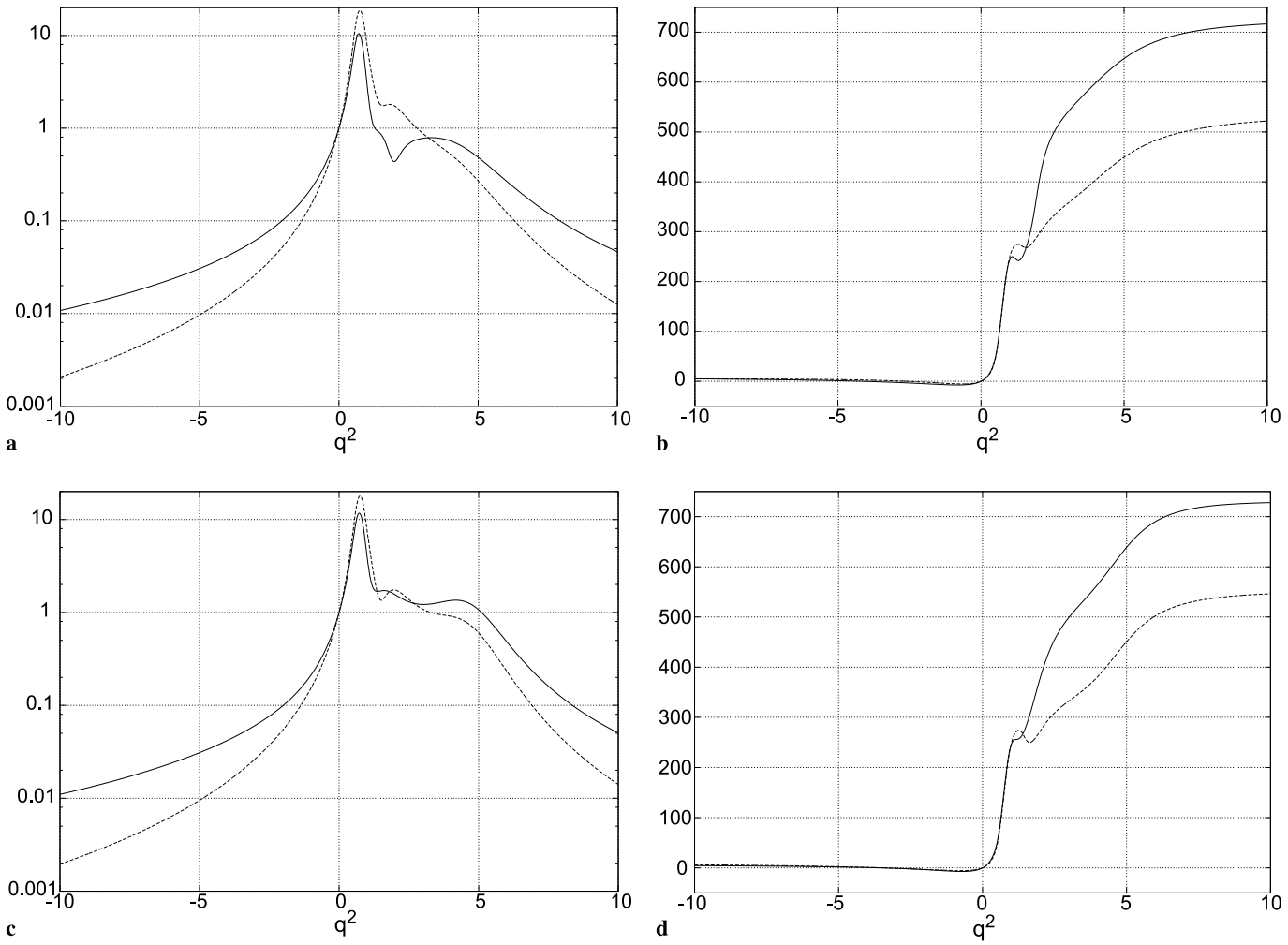

Fig. 6. Amplitude and phase of F_1 and F_2 for the two different models of $G_{\rm E}$: **a** amplitude of F_1 (*solid line*) and F_2 (*dashed line*) for model I, **b** phase (in degrees) of F_1 (*solid line*) and F_2 (*dashed line*) for model I, **c** amplitude of F_1 (*solid line*) and F_2 (*dashed line*) for model II and d phase (in degrees) of F_1 (*solid line*) and F_2 (*dashed line*) for model II

Using these models for the magnetic and electric form factors we can obtain the form factors F_1 and F_2, required for our calculation. The models used are convenient, since they allow us to use the Feynman parametrization to compute the loop integrals. The form factors for the two models have a small imaginary part even for space-like momenta. However, this region contributes negligibly to the loop integrals. The dominant contribution comes from the unphysical region $0 < q^2 < 4M_p^2$, where the form factor is several orders of magnitude larger than its value in the space-like region. In this region our model provides a very good fit to the extracted form factor [32]. Moreover, the imaginary part in the space-like region is very small and unlikely to affect our results significantly. The resulting amplitudes and phases for model I are shown in Fig. 6a and b respectively. The corresponding results for model II are shown in Fig. 6c and d.

Using the form-factor models in Appendix B we can determine the amplitudes of the box and cross box diagram as well as the amplitude due to the extra term displayed in (18). The box diagram amplitude can be written as

$$\begin{aligned}\mathrm{i}\mathcal{M}_{\rm B} = e^4 \sum_{a,b} \int \frac{\mathrm{d}^4 l}{(2\pi)^4} &\left[\frac{\bar{u}(k')\gamma^\mu(\not{k}' - \not{l})\gamma^\nu u(k)}{((k-l)^2 - m_e^2 + \mathrm{i}\xi)}\right] \\ &\times \left[\frac{1}{(l^2 - \mu^2 + \mathrm{i}\xi)(\tilde{q}^2 - \mu^2 + \mathrm{i}\xi)}\right] \\ &\times \left[\bar{U}(p')\left\{F_1(\tilde{q})\gamma_\mu + \mathrm{i}\frac{\kappa_p}{2M_p}F_2(\tilde{q})\sigma_{\mu\alpha}\tilde{q}^\alpha\right\}\right. \\ &\times \left\{\frac{\not{p} + \not{l} + M_p}{(p+l)^2 - M_p^2 + \mathrm{i}\xi}\right\} \\ &\left.\times \left\{F_1(l)\gamma_\nu + \mathrm{i}\frac{\kappa_p}{2M_p}F_2(l)\sigma_{\nu\beta}l^\beta\right\}U(p)\right], \quad (19)\end{aligned}$$

where $\tilde{q} = q - l$, m_e is the mass of the electron, and ξ is an infinitesimal positive parameter.[7] A small mass of the pho-

[7] Here we use the notation ξ instead of the standard notation ϵ to avoid confusion with the symbol ε used to denote the longitudinal polarization of the photon.

ton μ has been introduced in order to regulate the infrared divergence in these integrals. The infrared divergent part has to be subtracted from our result, since it is included in the standard radiative corrections that are applied while extracting the form factor. Using the form-factor model in Appendix B, we find

$$\begin{aligned}
\mathrm{i}\mathcal{M}_{\mathrm{B}} = e^4 \sum_{a,b} \int \frac{\mathrm{d}^4 l}{(2\pi)^4} & \left[\frac{\bar{u}(k')\gamma^\mu (\not{k}' - \not{l}) \gamma^\nu u(k)}{((k-l)^2 - m_e^2 + \mathrm{i}\xi)} \right] \\
& \times \left[\frac{1}{(l^2 - \mu^2 + \mathrm{i}\xi)(\tilde{q}^2 - \mu^2 + \mathrm{i}\xi)} \right] \\
& \times \Bigg[\bar{U}(p') \left\{ \left(C_a g_a(\tilde{q}) - 4M_p^2 D_a \tilde{g}_a(\tilde{q}) \right) \gamma_\mu \right. \\
& \left. + \left(\mathrm{i}2M_p D_a \tilde{g}_a(\tilde{q}) \right) \sigma_{\mu\alpha} \tilde{q}^\alpha \right\} \left\{ \frac{\not{p} + \not{l} + M_p}{(p+l)^2 - M_p^2 + \mathrm{i}\xi} \right\} \\
& \times \left\{ \left(C_b g_b(l) - 4M_p^2 D_b \tilde{g}_b(l) \right) \gamma_\nu \right. \\
& \left. + \left(\mathrm{i}2M_p D_b \tilde{g}_b(l) \right) \sigma_{\nu\beta} l^\beta \right\} U(p) \Bigg]. \qquad (20)
\end{aligned}$$

It is convenient to rewrite this expression in terms of the coefficients C' and D', defined in Appendix B. We find,

$$\begin{aligned}
\mathrm{i}\mathcal{M}_{\mathrm{B}} = e^4 \sum_{i,j} \int \frac{\mathrm{d}^4 l}{(2\pi)^4} & \left[\frac{\bar{u}(k')\gamma^\mu (\not{k}' - \not{l}) \gamma^\nu u(k)}{(k-l)^2 - m_e^2 + \mathrm{i}\xi} \right] \\
& \times \Bigg[\bar{U}(p') \Bigg\{ \Big(C_i' g_i(\tilde{q}) - 4M_p^2 D_i' g_i(\tilde{q}) \Big) \gamma_\mu \\
& + \Big(\mathrm{i}2M_p D_i' g_i(\tilde{q}) \Big) \sigma_{\mu\alpha} \tilde{q}^\alpha \Bigg\} \left\{ \frac{\not{p} + \not{l} + M_p}{(p+l)^2 - M_p^2 + \mathrm{i}\xi} \right\} \\
& \times \left\{ \Big(C_j' g_j(l) - 4M_p^2 D_j' g_j(l) \Big) \gamma_\nu \right. \\
& \left. + \Big(\mathrm{i}2M_p D_j' g_j(l) \Big) \sigma_{\nu\beta} l^\beta \right\} U(p) \Bigg] \qquad (21) \\
\equiv e^4 \int \frac{\mathrm{d}^4 l}{(2\pi)^4} & \left[\frac{1}{((k-l)^2 - m_e^2 + \mathrm{i}\xi)} \right] \\
& \times \left[\frac{1}{((p+l)^2 - M_p^2 + \mathrm{i}\xi)} \right] \\
& \times \sum_{i,j} \left[n_1(C_i', D_i', C_j', D_j') + l^4 n_2(C_i', D_i', C_j', D_j') \right],
\end{aligned}$$

where the last step defines the factors $n_1(C_i', D_i', C_j', D_j')$ and $n_2(C_i', D_i', C_j', D_j')$. We may cancel the l^2 factor multiplying $n_2(C_i', D_i', C_j', D_j')$ with a factor $(l^2 - \mu^2 + \mathrm{i}\xi)$ in the denominator. We then find

$$\begin{aligned}
\mathrm{i}\mathcal{M}_{\mathrm{B}} = e^4 \int \frac{\mathrm{d}^4 l}{(2\pi)^4} & \left[\frac{1}{((k-l)^2 - m_e^2 + \mathrm{i}\xi)} \right] \\
& \times \left[\frac{1}{((p+l)^2 - M_p^2 + \mathrm{i}\xi)} \right] \\
& \times \sum_{i,j} \left[n_1 \left(C_i' D_i', C_j', D_j' \right) + l^2 n_2 \left(C_i', D_i', C_j'', D_j'' \right) \right]. \qquad (22)
\end{aligned}$$

The cross box diagram amplitude is given by

$$\begin{aligned}
\mathrm{i}\mathcal{M}_{\mathrm{CB}} = e^4 \sum_{a,b} \int \frac{\mathrm{d}^4 l}{(2\pi)^4} & \left[\frac{\bar{u}(k')\gamma^\mu (\not{k}' - \not{l}) \gamma^\nu u(k)}{(k-l)^2 - m_e^2 + \mathrm{i}\xi} \right] \\
& \times \left[\frac{1}{(l^2 - \mu^2 + \mathrm{i}\xi)(\tilde{q}^2 - \mu^2 + \mathrm{i}\xi)} \right] \\
& \times \left[\bar{U}(p') \left\{ F_1(l)\gamma_\nu + \mathrm{i}\frac{\kappa_p}{2M_p} F_2(l) \sigma_{\nu\beta} l^\beta \right\} \right. \\
& \times \left\{ \frac{\not{p} + \not{q} - \not{l} + M_p}{(p+\tilde{q})^2 - M_p^2 + \mathrm{i}\xi} \right\} \\
& \left. \times \left\{ F_1(\tilde{q})\gamma_\mu + \mathrm{i}\frac{\kappa_p}{2M_p} F_2(\tilde{q}) \sigma_{\mu\alpha} \tilde{q}^\alpha \right\} U(p) \right]. \qquad (23)
\end{aligned}$$

Using the form-factor model given in Appendix B it can be written as

$$\begin{aligned}
\mathrm{i}\mathcal{M}_{\mathrm{CB}} = e^4 \sum_{a,b} \int \frac{\mathrm{d}^4 l}{(2\pi)^4} & \left[\frac{\bar{u}(k')\gamma^\mu (\not{k}' - \not{l}) \gamma^\nu u(k)}{(k-l)^2 - m_e^2 + \mathrm{i}\xi} \right] \\
& \times \left[\frac{1}{(l^2 - \mu^2 + \mathrm{i}\xi)(\tilde{q}^2 - \mu^2 + \mathrm{i}\xi)} \right] \\
& \times \Bigg[\bar{U}(p') \Bigg\{ \Big(C_b g_b(l) - 4M_p^2 D_b \tilde{g}_b(l) \Big) \gamma_\nu \\
& + \Big(\mathrm{i}2M_p D_b \tilde{g}_b(l) \Big) \sigma_{\nu\beta} l^\beta \Bigg\} \left\{ \frac{\not{p} + \not{q} - \not{l} + M_p}{(p+\tilde{q})^2 - M_p^2 + \mathrm{i}\xi} \right\} \\
& \times \left\{ \Big(C_a g_a(\tilde{q}) - 4M_p^2 D_a \tilde{g}_a(\tilde{q}) \Big) \gamma_\mu \right. \\
& \left. + \Big(\mathrm{i}2M_p D_a \tilde{g}_a(\tilde{q}) \Big) \sigma_{\mu\alpha} \tilde{q}^\alpha \right\} U(p) \Bigg]. \qquad (24)
\end{aligned}$$

The amplitude proportional to $\bar{b}^2$ is given by

$$\begin{aligned}
\mathrm{i}\mathcal{M}_{\bar{b}} = \left(\frac{e^4 \bar{b}^2}{8M_p^2} \right) \sum_{a,b} \int \frac{\mathrm{d}^4 l}{(2\pi)^4} & \left[\frac{\bar{u}(k')\gamma^\mu (\not{k}' - \not{l}) \gamma^\nu u(k)}{(k-l)^2 - m_e^2 + \mathrm{i}\xi} \right] \\
& \times \left[\frac{1}{(l^2 - \mu^2 + \mathrm{i}\xi)(\tilde{q}^2 - \mu^2 + \mathrm{i}\xi)} \right] \\
& \times \Bigg[\bar{U}(p') \Bigg\{ \left(\frac{\mathrm{i}\kappa_p}{2M_p} F_2(\tilde{q}) \sigma_{\mu\alpha} (\tilde{q})^\alpha \right) (\not{p} + \not{l} - M_p) \\
& \times \left(\frac{\mathrm{i}\kappa_p}{2M_p} F_2(l) \sigma_{\nu\beta} l^\beta \right) + \left(\frac{\mathrm{i}\kappa_p}{2M_p} F_2(l) \sigma_{\nu\beta} l^\beta \right) \\
& \times (\not{p} + \not{q} - \not{l} - M_p) \left(\frac{\mathrm{i}\kappa_p}{2M_p} F_2(\tilde{q}) \sigma_{\mu\alpha} \tilde{q}^\alpha \right) \Bigg\} U(p) \Bigg]
\end{aligned}$$

$$
\begin{aligned}
&= \left(\frac{e^4\bar{b}^2}{8M_p^2}\right)\sum_{i,j}\int\frac{\mathrm{d}^4l}{(2\pi)^4}\left[\frac{\bar{u}(k')\gamma^\mu(\not{k}'-\not{l})\gamma^\nu u(k)}{(k-l)^2-m_e^2+\mathrm{i}\xi}\right]\\
&\quad\times\left[\bar{U}(p')\left\{(\mathrm{i}2M_pD_i'g_i(\tilde{q})\sigma_{\mu\alpha}\tilde{q}^\alpha)\,(\not{p}'+\not{l}-M_p)\right.\right.\\
&\quad\times\left(\mathrm{i}2M_pD_j'g_j(l)\sigma_{\nu\beta}l^\beta\right)+\left(\mathrm{i}2M_pD_j'g_j(l)\sigma_{\nu\beta}l^\beta\right)\\
&\quad\left.\left.\times(\not{p}+\not{q}-\not{l}-M_p)\,(\mathrm{i}2M_pD_i'g_i(\tilde{q})\sigma_{\mu\alpha}\tilde{q}^\alpha)\right\}U(p)\right].
\end{aligned}
$$

In our numerical calculation we set the mass of the electron $m_e = 0$.

The contribution of the two-photon exchange diagrams to the electron–proton elastic scattering cross section can be written as

$$
\frac{\mathrm{d}\sigma^{2\gamma}}{\mathrm{d}\Omega_e} = \frac{2\,\mathrm{Re}(\overline{\mathcal{M}_0^*\mathcal{M}_{2\gamma}})E_e'^2}{64M_p^2\pi^2E_e^2} + \mathcal{O}(\alpha^4)\,, \tag{25}
$$

where

$$
\mathcal{M}_{2\gamma} = \mathcal{M}_\mathrm{B} + \mathcal{M}_\mathrm{CB} + \mathcal{M}_{\bar{b}} \tag{26}
$$

is the total amplitude of the two-photon exchange diagrams, and

$$
\begin{aligned}
\mathcal{M}_0 = &-\frac{e^2}{q^2}\bar{u}(k')\gamma^\mu u(k)\bar{U}(p')\\
&\times\left(F_1(q)\gamma_\mu + \frac{\mathrm{i}\kappa_p}{2M_p}F_2(q)\sigma_{\mu\alpha}q^\alpha\right)U(p)
\end{aligned} \tag{27}
$$

is the tree amplitude. Hence, the contribution of the two-photon exchange diagrams to the reduced cross section is given by

$$
\begin{aligned}
\sigma_\mathrm{R}^{2\gamma} &= \frac{\varepsilon(1+\tau)}{\sigma_\mathrm{Mott}}\frac{\mathrm{d}\sigma^{2\gamma}}{\mathrm{d}\Omega_e}\\
&= \left(\frac{4E_e^3\sin^4\frac{\theta_e}{2}}{\alpha^2E_e'\cos^2\frac{\theta_e}{2}}\right)\varepsilon(1+\tau)\left(\frac{2\,\mathrm{Re}\left(\overline{\mathcal{M}_0^*\mathcal{M}_{2\gamma}}\right)E_e'^2}{64M_p^2\pi^2E_e^2}\right)\\
&= \frac{q^4\varepsilon(1+\tau)}{32\alpha^2\pi^2M_p^2(q^2+4E_eE_e')}\,\mathrm{Re}\left(\overline{\mathcal{M}_0^*\mathcal{M}_{2\gamma}}\right).
\end{aligned} \tag{28}
$$

The diagram proportional to $\bar{b}^2$ has no infrared (IR) divergent term. So the contribution coming from it is computed keeping $\mu^2 = 0$. Contributions from box and cross box diagrams are computed at 10 different values of μ^2 (from 0.005 to 0.0095). The numerical calculation of the cross box diagram is straightforward since the integral is well defined. However, for the evaluation of the box diagram the numerical evaluation is facilitated by keeping a small imaginary term ξ in the propagators. This makes the integral in the infrared limit well defined in the case $m_e = 0$. For each value of q^2, ε and μ^2, we have calculated the box diagram amplitude for 4 different values of ξ (between 0.001 and 0.00175). The amplitudes depend almost linearly on ξ. The final μ^2 dependent box diagram amplitudes are obtained by extrapolation to $\xi = 0$. The two different models for the form factors described in Appendix B give almost identical results. So for the rest of the section we quote the result obtained using model-I only.

The IR behavior of the two-photon diagrams has been calculated by Mo and Tsai [18, 19]. In the limit $\mu^2 \to 0$ the leading term from the box and cross box diagram can be expressed as

$$
\mathcal{M}_\mathrm{IR}^{2\gamma} = \frac{\alpha}{\pi}[K(p',k) - K(p,k)]\mathcal{M}_0\,, \tag{29}
$$

where

$$
\begin{aligned}
K(p_i,p_j) = (p_i.p_j)&\int_0^1\frac{\mathrm{d}x}{(xp_i+(1-x)p_j)^2}\\
&\times\ln\left[\frac{(xp_i+(1-x)p_j)^2}{\mu^2}\right].
\end{aligned}
$$

The IR contribution to the reduced cross section coming from the box and cross box diagram is given by

$$
\sigma_\mathrm{IR}^{2\gamma} = \frac{2\alpha}{\pi}[K(p',k) - K(p,k)]\sigma_\mathrm{R}^{1\gamma}\,. \tag{30}
$$

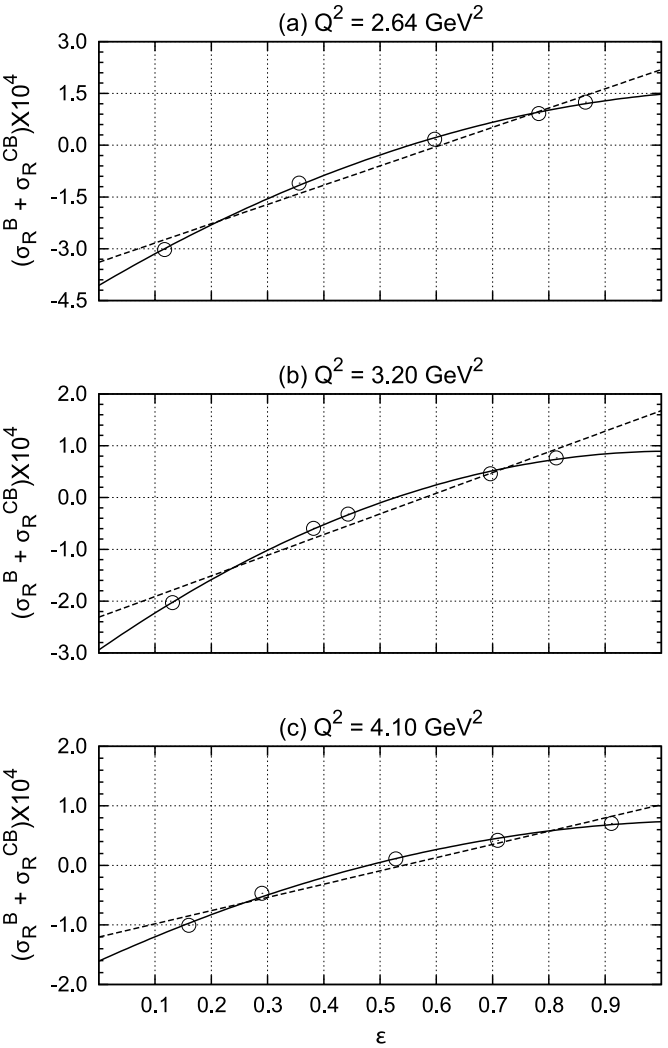

Fig. 7. Total contribution of the box and cross box diagram to the elastic electron–proton scattering for $Q^2 = 2.64\,\mathrm{GeV}^2$ **a**, $3.20\,\mathrm{GeV}^2$ **b**, $4.10\,\mathrm{GeV}^2$ **c**. The *dashed lines* represent f_1, see (33), and the *solid curves* represent f_2, see (34). The fitting parameters are given in Table 1

Let

$$\sigma_{\rm IR}^{2\gamma} \equiv a_{\rm ir} + b_{\rm ir} \ln \mu^2 \,. \tag{31}$$

To remove the IR part from $\sigma_{\rm R}^{2\gamma}$ we fit it with the following function:

$$\sigma_{\rm R}^{2\gamma} = a(\mu^2) + b(\mu^2) \ln \mu^2 \,, \tag{32}$$

with

$$a(\mu^2) = a_0 + a_{\rm ir} + a_1\mu^2 + \mathcal{O}[\mu^4] \,,$$
$$b(\mu^2) = b_{\rm ir} + b_1\mu^2 + \mathcal{O}[\mu^4] \,.$$

Here a_0 gives the IR removed $\sigma_{\rm R}^{2\gamma}$. It has been explicitly verified that keeping $\mathcal{O}[\mu^4]$ terms in $a(\mu)$ and $b(\mu)$ has no effect on the slope (and thus on $G_{\rm E}$) of $\sigma_{\rm R}^{2\gamma}(\varepsilon)$ with respect to ε. The difference between these two fits leads to a very small correction to $G_{\rm M}$ only and hence can be ignored.

The result of the calculation for the box and cross box diagrams is given in Figs. 7 and 8. Here we have considered the momentum transfer $Q^2 = 2.64,\ 3.20,\ 4.10,\ 5.00$ and $6.00\,{\rm GeV}^2$. The first three values are the same as those used in the JLAB extraction of form factors using the Rosenbluth separation. The contribution from the diagram proportional to $\bar{b}^2$ is shown in Figs. 9 and 10. Here $\bar{b}$ is taken as 1. We fit $\sigma_{\rm R}^{\rm BCB} \equiv (\sigma_{\rm R}^{\rm B} + \sigma_{\rm R}^{\rm CB})$ and $\sigma_{\rm R}^{\bar{b}}$ (here and for rest of the section we use the notation $\sigma_{\rm R}^{2\gamma}$ and $\sigma_{\rm R}^{\rm BCB}$ to denote the IR removed contributions) to the following functions:

$$f_1(\varepsilon) = c_1 + c_2\varepsilon \,, \tag{33}$$
$$f_2(\varepsilon) = d_1 + d_2\varepsilon + d_3\varepsilon^2 \,. \tag{34}$$

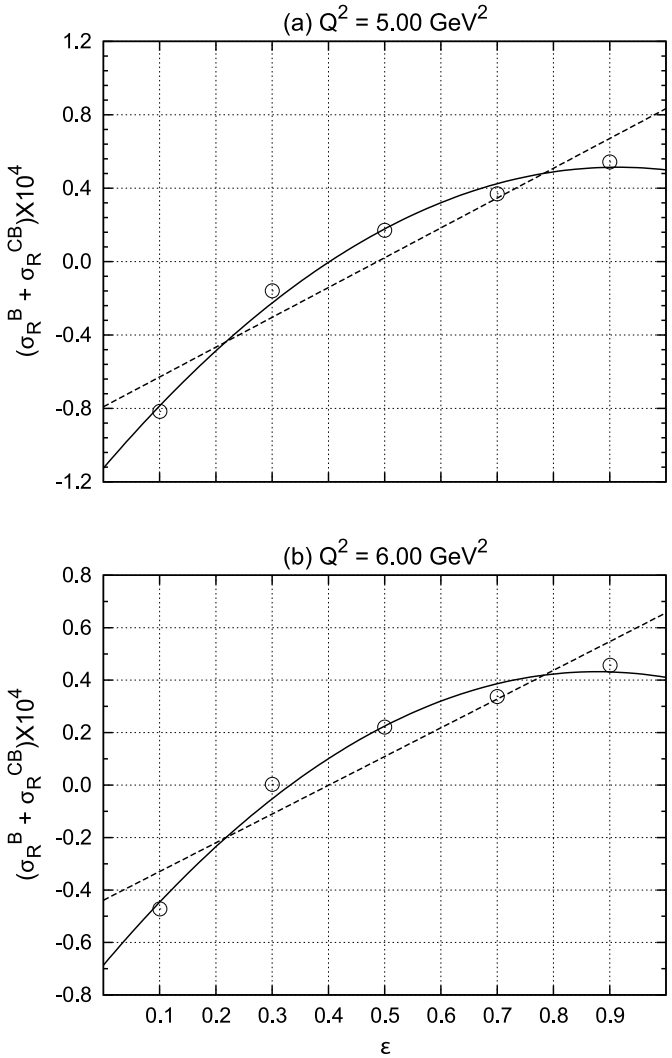

Fig. 8. Total contribution of the box and cross box diagram to the elastic electron– proton scattering for $Q^2 = 5\,{\rm GeV}^2$ **a**, $6\,{\rm GeV}^2$ **b**. The *dashed lines* represent f_1, see (33), and the *solid curves* represent f_2, see (34). The fitting parameters are given in Table 1

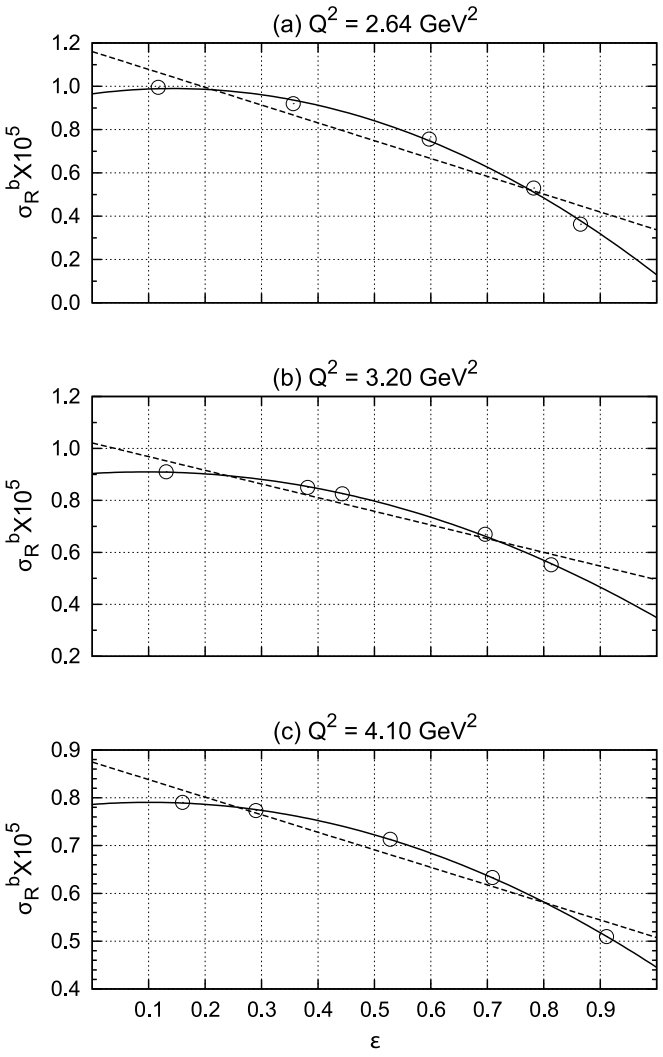

Fig. 9. Contribution of the diagram proportional to $\bar{b}^2$ to the elastic electron proton scattering for $Q^2 = 2.64\,{\rm GeV}^2$ **a**, $3.20\,{\rm GeV}^2$ **b**, $4.10\,{\rm GeV}^2$ **c**. Here $\bar{b} = 1$. The *dashed lines* represent f_1, see (33), and the *solid curves* represent f_2, see (34). The fitting parameters are given in Table 2

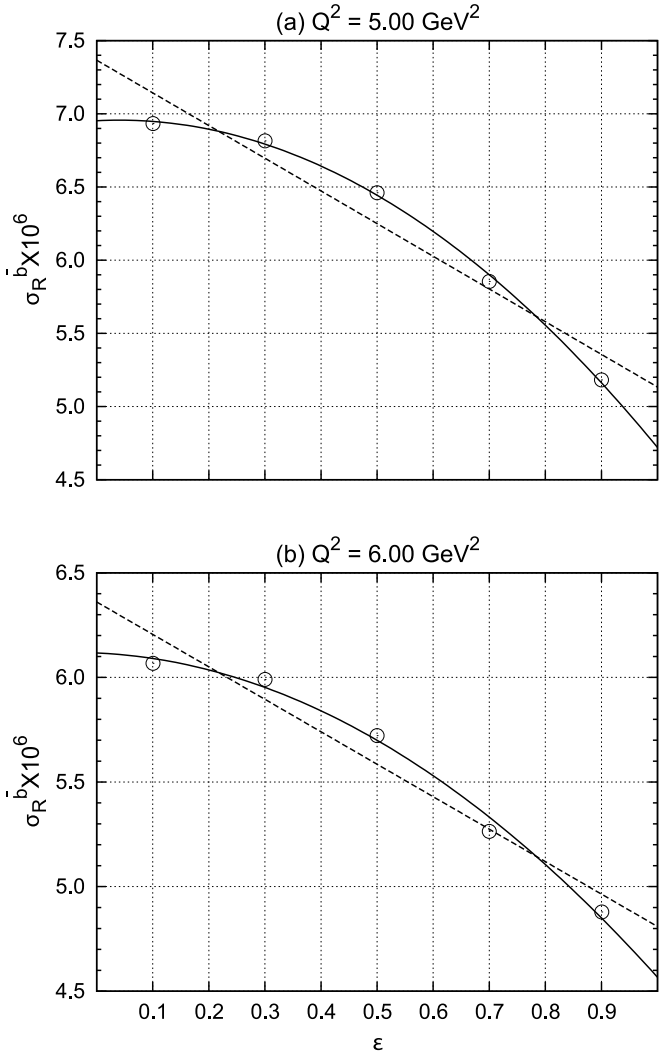

Fig. 10. Contribution of the diagram proportional to $\bar{b}^2$ to the elastic electron–proton scattering for $Q^2 = 5\ \mathrm{GeV}^2$ **a**, $6\ \mathrm{GeV}^2$ **b**. Here $\bar{b} = 1$. The *dashed lines* represent f_1, see (33), and the *solid curves* represent f_2, see (34). The fitting parameters are given in Table 2

The values of c_1, c_2 and d_1, d_2, d_3 for $\sigma_{\mathrm{R}}^{\mathrm{BCB}}$ and $\sigma_{\mathrm{R}}^{\bar{b}}$ are given in Tables 1 and 2, respectively. From Tables 1 and 2 we also see that the contribution due to the $\bar{b}$ term is relatively small as long as the magnitude of $\bar{b}$ is of order unity. As the magnitude of $\bar{b}$ is unknown we shall assume $\bar{b} \approx 0$ and take $\sigma_{\mathrm{R}}^{2\gamma} \approx \sigma_{\mathrm{R}}^{\mathrm{BCB}}$ for the rest of the section.

Figure 11 shows the contribution of the dimension five operator proportional to F_2 to the reduced cross section. This contribution is obtained from the box and cross box diagrams. For comparison we also show the total contribution of both these diagrams. The IR μ^2 dependence is not removed in this calculation and the parameters chosen are $Q^2 = 4.10\ \mathrm{GeV}^2$ and $\mu^2 = 0.005\ \mathrm{GeV}^2$. We find that the contribution from terms proportional to $F_2 \times F_2$ is much smaller compared to the total contribution, justifying the truncation of our action to only operators of dimension five.

To obtain the corrected σ_{R} we subtract the linear fit to $\sigma_{\mathrm{R}}^{2\gamma}$ and $f_1^{2\gamma}(\varepsilon)$ (see (33) and Table 1), from a linear fit to

Table 1. Values of fitting parameters for $(\sigma_{\mathrm{R}}^{\mathrm{B}} + \sigma_{\mathrm{R}}^{\mathrm{CB}})$. All numbers have been scaled by 10^4. The parameters c_1 and c_2 are defined at (33) and d_1, d_2 and d_3 are defined at (34). The standard errors obtained in fitting the result are also shown. Figures 7 and 8 show the functions f_1 and f_2 for this case

Q^2	c_1	c_2	d_1	d_2	d_3
2.64	−3.39	5.59	−4.06	9.58	−4.04
	±0.30	±0.48	±0.12	±0.59	±0.58
3.20	−2.31	3.99	−2.94	7.53	−3.69
	±0.25	±0.45	±0.08	±0.38	±0.38
4.10	−1.20	2.23	−1.61	4.30	−1.95
	±0.15	±0.25	±0.11	±0.47	±0.43
5.00	−0.79	1.63	−1.13	3.59	−1.96
	±0.16	±0.28	±0.10	±0.47	±0.46
6.00	−0.44	1.10	−0.69	2.55	−1.45
	±0.12	±0.21	±0.08	±0.40	±0.39

Table 2. Values of fitting parameters for $\sigma_{\mathrm{R}}^{\bar{b}}$ with $\bar{b} = 1$. All numbers have been scaled by 10^6. The standard errors obtained in fitting the result are also shown. The parameters c_1 and c_2 are defined at (33) and d_1, d_2 and d_3 are defined at (34). Figures 9 and 10 show the functions f_1 and f_2 for this case

Q^2	c_1	c_2	d_1	d_2	d_3
2.64	11.60	−8.23	9.65	3.37	−11.73
	±0.86	±1.41	±0.37	±1.81	±1.79
3.20	10.21	−5.27	9.04	1.29	−6.84
	±0.45	±0.83	±0.12	±0.59	±0.60
4.10	8.75	−3.67	7.86	0.86	−4.27
	±0.31	±0.52	±0.04	±0.16	±0.14
5.00	7.37	−2.23	6.95	0.20	−2.43
	±0.19	±0.34	±0.06	±0.29	±0.28
6.00	6.36	−1.55	6.12	−0.12	−1.43
	±0.12	±0.21	±0.09	±0.44	±0.42

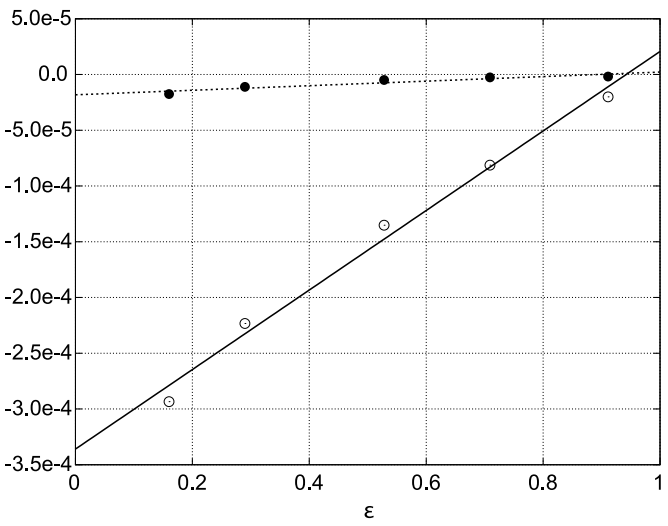

Fig. 11. The contribution to the reduced cross section coming from terms proportional to $F_2(l)F_2(q-l)$ in $\mathcal{M}_{\mathrm{CB}}$ and $\mathcal{M}_{\mathrm{B}}$ for $Q^2 = 4.10\ \mathrm{GeV}^2$ and $\mu^2 = 0.005\ \mathrm{GeV}^2$ (*filled circles*). The *unfilled circles* represent the total contribution coming from both the form factors F_1 and F_2 for the same Q^2 and μ^2

$\sigma_{\rm R}^{\rm LT}(\varepsilon)$ given by

$$\sigma_{\rm R}^{\rm LT}(\varepsilon) = \mathcal{G}_0(1+\varepsilon\mathcal{G}_1)\,. \tag{35}$$

Then the corrected reduced cross section is

$$\begin{aligned}\bar{\sigma}_{\rm R}(\varepsilon) &\equiv \sigma_{\rm R}^{\rm LT} - \sigma_{\rm R}^{2\gamma} \\ &= \left(\mathcal{G}_0 - c_1^{2\gamma}\right) + \varepsilon\left(\mathcal{G}_0\mathcal{G}_1 - c_2^{2\gamma}\right). \end{aligned} \tag{36}$$

In Fig. 12 we plot $\bar{\sigma}_{\rm R}(\varepsilon)$ for different Q^2. We determine the corrected form factors $\bar{G}_{\rm M}$ and $\bar{G}_{\rm E}$ by

$$\bar{G}_{\rm M} = \frac{1}{\tau}\sqrt{\mathcal{G}_0 - c_1^{2\gamma}}\,, \tag{37}$$

$$\bar{G}_{\rm E} = \sqrt{\mathcal{G}_0\mathcal{G}_1 - c_2^{2\gamma}}. \tag{38}$$

Figure 13 shows how the ratio $\mu_p G_{\rm E}/G_{\rm M}$ is modified by the two-photon exchange contributions. The SLAC Rosenbluth data after applying the two-photon exchange correction are shown by the unfilled circles. The dotted line represents the best linear fit through these data. We find that the two-photon exchange correction completely explains the difference between the SLAC Rosenbluth separation data and the JLAB polarization transfer data. However, it is not able to explain the difference between the JLAB Rosenbluth and polarization transfer results. The corrected JLAB Rosenbluth data are shown by filled circles. The JLAB Rosenbluth data lie systematically above the SLAC data.

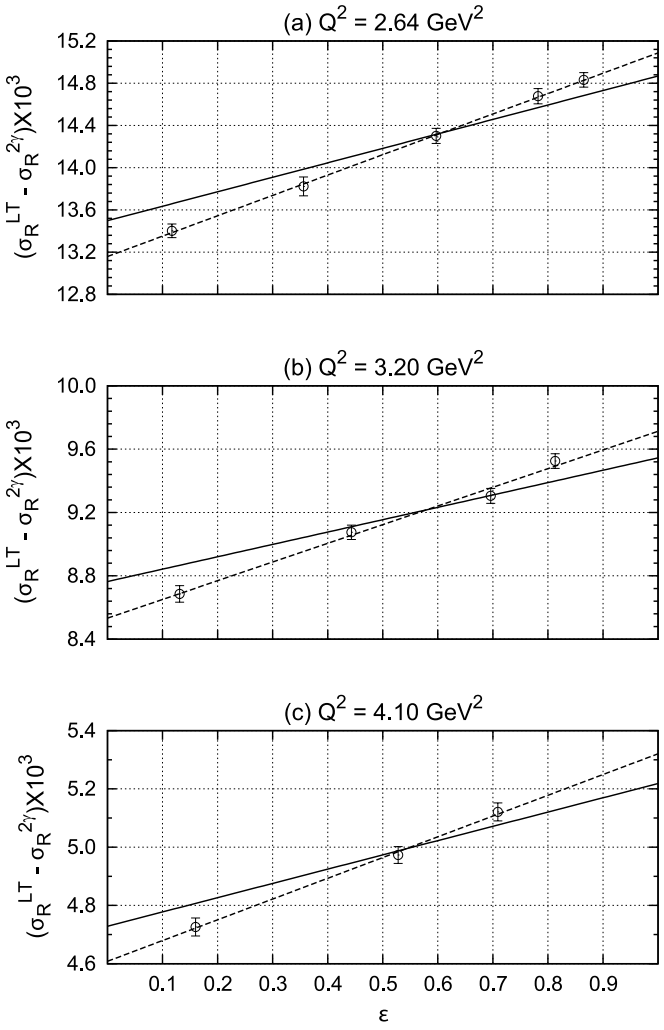

Fig. 12. Corrected cross section, $\bar{\sigma}_{\rm R}$ (*solid lines*) obtained using (15) with $\bar{b}=0$ for $Q^2 = 2.64\,{\rm GeV}^2$ **a**, $3.20\,{\rm GeV}^2$ **b**, $4.10\,{\rm GeV}^2$ **c**. The *unfilled circles* represent the data points obtained by the Rosenbluth separation method at JLAB and the *dashed lines* are the *straight line* fits to these

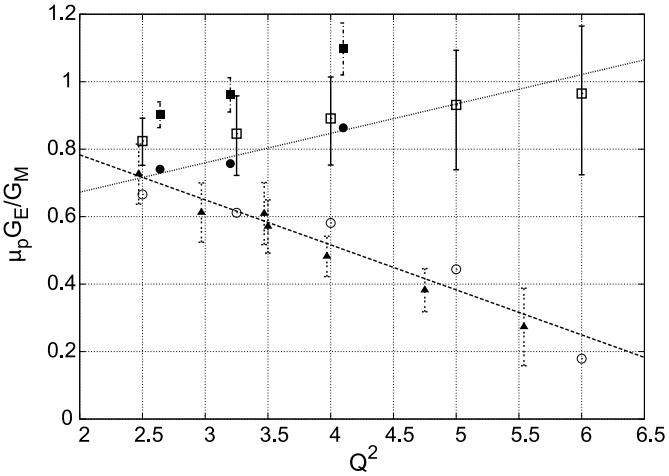

Fig. 13. The ratio $\mu_p G_{\rm E}/G_{\rm M}$ obtained by the polarization transfer technique at JLAB (*filled triangles*) and the Rosenbluth separation technique at SLAC (*unfilled squares*) and JLAB (*filled squres*). The ratio after correcting for the two-photon exchange contribution is also shown. The *filled circles* are the corrected JLAB Rosenbluth data and the *dotted line* is the best fit through these points. The *unfilled circles* are the corrected SLAC Rosenbluth data and the *dashed line* is the best fit through these points

7 Conclusions

In this paper we have constructed a non-local Lagrangian to model the electromagnetic interaction of the proton. The model is invariant under a non-local form of gauge transformations and incorporates all operators up to dimension five. The model displays the standard electromagnetic vertex of an on-shell proton. The dimension five operators also contain an operator with an unknown coefficient, whose value can be extracted experimentally. We use this model to compute the two-photon exchange diagrams contributing to elastic scattering of an electron with a proton. The calculation requires the proton form factors in the entire kinematic range. We find that the two-photon exchange diagram contribution to the reduced cross section $\sigma_{\rm R}$ shows a slightly non-linear dependence on the longitudinal polarization of the photon ε. The non-linearity seen is within the experimental error bars of the Rosenbluth data. We apply the correction due to two-photon exchange

contributions to both the SLAC and JLAB Rosenbluth separation data. The resulting cross section for the SLAC data is completely consistent with the JLAB polarization transfer results. However, the JLAB Rosenbluth data still show a large deviation. It, therefore, appears that the two-photon exchange is able to explain the difference in the experimental extraction of proton electromagnetic form factor $G_{\rm E}$ using the Rosenbluth separation and polarization transfer techniques if we accept the SLAC Rosenbluth data, which are available over a larger momentum range. Similar trends have also be observed in the two-photon exchange contributions obtained in [23–25, 27].

Appendix A

We shall show in this appendix that the first term in (18) proportional to

$$\overline{\psi}' \left(\sigma_{\mu\nu} f_2' \left[\frac{\partial^2}{\Lambda^2} \right] F^{\mu\nu} \right)^2 \psi'$$

does not contribute to the two-photon matrix element in the one-loop approximation in the Feynman gauge in the zero electron mass limit $m_e = 0$. For this purpose we write the term as

$$\frac{1}{2}\overline{\psi}' \left(\sigma_{\mu\nu}\sigma_{\lambda\rho} + \sigma_{\lambda\rho}\sigma_{\mu\nu}\right) f_2' \left[\frac{\partial^2}{\Lambda^2} \right] F^{\mu\nu} f_2' \left[\frac{\partial^2}{\Lambda^2} \right] F^{\lambda\rho} \psi' \,.$$

We then note the following.

- $\sigma_{\mu\nu}\sigma_{\lambda\rho} + \sigma_{\lambda\rho}\sigma_{\mu\nu}$ is a linear combination of $\mathbb{I}$ and $\gamma_5 = \alpha \left(g_{\mu\lambda}g_{\nu\rho} - g_{\mu\rho}g_{\nu\lambda}\right)\mathbb{I} + \mathrm{i}\beta\xi_{\mu\nu\lambda\rho}\gamma_5$, where α, β are constants and, in particular, *no* σ terms appear.
- The Feynman integral has no dependence on both p and p'.
- Thus, the result for the two-photon exchange diagram is of the form

$$\overline{u}(k')\gamma_\mu\gamma_\alpha\gamma_\nu u(k)\overline{U}(p')[\mathbb{I}, \gamma_5]U\,(p) \times I^{\mu\alpha\nu}(k, k')\,.$$

On simplification, this becomes

$$\overline{u}(k')\left\{g_{\mu\alpha}\gamma_\nu + g_{\nu\alpha}\gamma_\mu - g_{\mu\nu}\gamma_\alpha + 4\mathrm{i}\xi_{\mu\alpha\nu\beta}\gamma^\beta\gamma_5\right\}u(k) \times \overline{U}(p')[\mathbb{I}, \gamma_5]U\,(p) \times I^{\mu\alpha\nu}(k, k')\,.$$

Now, $g_{\mu\alpha}I^{\mu\alpha\nu}(k, k')$ is a linear combination of terms that are $\sim k^\nu$ or k'^ν. Both of these terms give zero. Similar logic applies to all other terms.

Appendix B: Model for the form factors

The fits for $G_{\rm M}/\mu_p$ and $G_{\rm E}$ are given by

$$\frac{G_{\rm M}(q^2)}{\mu_p} = \sum_{a=1}^{4} \frac{A_a^{'}}{(q^2 - m_a^2 + \mathrm{i}m_a\Gamma_a')}\,, \qquad \text{(B.1)}$$

$$G_{\rm E}(q^2) = \sum_{a=1}^{6} \frac{B_a^{'}}{(q^2 - m_a^2 + im_a\Gamma_a')}\,. \qquad \text{(B.2)}$$

We have considered two fits for $G_{\rm E}$. The values of the masses and the parameters are tabulated in Table 3 (model I) and Table 4 (model II).

Using the models for the magnetic and electric form factors we can determine the Dirac and Pauli form factors. Let the fits to the form factors $G_{\rm M}$ and $G_{\rm E}$ be

$$G_{\rm M}(q^2) = \sum_{a=1}^{6} A_a g_a(q^2)\,, \qquad \text{(B.3)}$$

$$G_{\rm E}(q^2) = \sum_{a=1}^{6} B_a g_a(q^2)\,, \qquad \text{(B.4)}$$

with $A_a = \mu_p A_a^{'}$ and $B_a = B_a^{'}$. The g_a are defined by

$$g_a(q^2) = \frac{1}{q^2 - m_a^2 + \mathrm{i}\Gamma_a}\,. \qquad \text{(B.5)}$$

Table 3. Masses, widths and parameter values for $G_{\rm M}/\mu_p$ and $G_{\rm E}$ fits (model I). The $A^{'}$ and $B^{'}$ are defined in (B.1) and (B.2)

a	$A_a^{'}$	$B_a^{'}$	m_a	$\Gamma_a^{'}$
1	-2.882564 $+\mathrm{i}\,1.944314$	-3.177877 $+\mathrm{i}\,2.123389$	0.8084	0.2226
2	2.882564 $-\mathrm{i}\,1.944314$	3.177877 $-\mathrm{i}\,2.123389$	0.9116	0.1974
3	-1.064011 $-\mathrm{i}\,3.216318$	-0.608148 $-\mathrm{i}\,5.685885$	1.274	0.5712
4	1.064011 $+\mathrm{i}\,3.216318$	0.608148 $+\mathrm{i}\,5.685885$	1.326	0.5488
5	0	3.211388 $+\mathrm{i}\,0.693412$	1.96	1.02
6	0	$-\mathrm{i}\,0.693412$ $-\mathrm{i}\,0.693412$	2.04	0.98

Table 4. Masses, widths and parameter values for $G_{\rm M}/\mu_p$ and $G_{\rm E}$ fits (model II). The $A^{'}$ and $B^{'}$ are defined in (B.1) and (B.2)

a	$A_a^{'}$	$B_a^{'}$	m_a	$\Gamma_a^{'}$
1	-2.882564 $+\mathrm{i}\,1.944314$	-3.392256 $+\mathrm{i}\,2.194129$	0.8084	0.2226
2	2.882564 $-\mathrm{i}\,1.944314$	3.392256 $-\mathrm{i}\,2.194129$	0.9116	0.1974
3	-1.064011 $-\mathrm{i}\,3.216318$	1.224037 $-\mathrm{i}\,6.877523$	1.274	0.5712
4	1.064011 $+\mathrm{i}\,3.216318$	-1.224037 $+\mathrm{i}\,6.877523$	1.326	0.5488
5	0	1.645805 $+\mathrm{i}\,1.824298$	2.107	0.663
6	0	-1.645805 $-\mathrm{i}\,1.824298$	2.193	0.637

The form factors, F_1 and F_2, are given by

$$\kappa_p F_2 = \frac{G_{\rm M} - G_{\rm E}}{1+\tau} = 4M_p^2 \frac{G_{\rm E} - G_{\rm M}}{q^2 - 4M_p^2} = \sum_a 4M_p^2 D_a \tilde{g}_a \,, \tag{B.6}$$

$$F_1 = G_{\rm M} - \kappa_p F_2 = \sum_{a=1}^{6} \left(C_a g_a - 4M_p^2 D_a \tilde{g}_a \right), \tag{B.7}$$

where $C_a = A_a$, $D_a = B_a - A_a$ and $\tilde{g}_a = g_a / \left(q^2 - 4M_p^2\right)$. These definitions are convenient in evaluating the two-photon exchange amplitudes. We also have

$$\frac{\kappa_p F_2}{q^2 - \mu^2 + {\rm i}\xi} = \sum_{a=1}^{6} \frac{4M_p^2 D_a}{(q^2 - \mu^2 + {\rm i}\xi)(q^2 - 4M_p^2)(q^2 - m_a^2 + {\rm i}\Gamma_a)} \tag{B.8}$$

$$= \sum_{i=1}^{8} \frac{4M_p^2 D_i'}{q^2 - m_i^2 + {\rm i}\Gamma_i} \,, \tag{B.9}$$

with $m_7 = \mu$, $m_8 = 2M_p$, $\Gamma_7 = \xi$ and $\Gamma_8 = 0$. Here ($a = 1, 2, ..., 6$)

$$D_a' = \left[\frac{1}{m_a^2 - 4M_p^2 - {\rm i}\Gamma_a} - \frac{1}{m_a^2 - \mu^2 + {\rm i}\xi - {\rm i}\Gamma_a} \right] \times \frac{D_a}{\left(4M_p^2 - \mu^2 + {\rm i}\xi\right)} \,,$$

$$D_7' = \sum_{a=1}^{6} \frac{D_a}{\left(4M_p^2 - \mu^2 + {\rm i}\xi\right)\left(m_a^2 - \mu^2 + {\rm i}\xi - {\rm i}\Gamma_a\right)} \,,$$

$$D_8' = -\sum_{a=1}^{6} \frac{D_a}{\left(4M_p^2 - \mu^2 + {\rm i}\xi\right)\left(m_a^2 - 4M_p^2 - {\rm i}\Gamma_a\right)} = 0 \,.$$

The coefficient D_8' is found to be zero, and hence the summation in (B.9) terminates at $i = 7$. Similarly,

$$\frac{F_1}{q^2 - \mu^2 + {\rm i}\xi} = \sum_{i=1}^{8} \frac{C_i' - 4M_p^2 D_i'}{q^2 - m_i^2 + {\rm i}\Gamma_i} \,, \tag{B.10}$$

where

$$C_a' = \frac{C_a}{m_a^2 - \mu^2 + {\rm i}\xi - {\rm i}\Gamma_a} \,,$$

$$C_7' = -\sum_{a=1}^{6} \frac{C_a}{m_a^2 - \mu^2 + {\rm i}\xi - {\rm i}\Gamma_a} \,,$$

$$C_8' = 0.$$

We can also write F_1 and $\kappa_p F_2$ using this general notation. We find

$$\kappa_p F_2 = \sum_{i=1}^{7} \frac{4M_p^2 D_i''}{q^2 - m_i^2 + {\rm i}\Gamma_i} \,, \tag{B.11}$$

$$F_1 = \sum_{i=1}^{7} \frac{C'' - 4M_p^2 D_i''}{q^2 - m_i^2 + {\rm i}\Gamma_i} \,, \tag{B.12}$$

with

$$D_a'' = \frac{D_a}{m_a^2 - 4M_p^2 + {\rm i}\xi - {\rm i}\Gamma_a} \,,$$

$$D_7'' = 0 \,,$$

$$C_a'' = A_a \,,$$

$$C_7'' = 0 \,.$$

Appendix C: Sample calculation: box diagram

Here we present a sample calculation of one of the terms in the box diagram. The contribution of the box diagram amplitude to the two-photon exchange cross section is proportional to

$$\overline{\mathcal{M}_0^* \mathcal{M}_{\rm B}'} = {\rm i}\frac{e^6}{q^2} \sum_{i,j} \mathcal{I}_{\rm B}^{ij} \,, \tag{C.1}$$

where,

$$\mathcal{I}_{\rm B}^{ij} = \int \frac{{\rm d}^4 l}{(2\pi)^4} \frac{\mathcal{N}^{ij}(l)}{((k-l)^2 - m_e^2 + {\rm i}\xi)(l^2 - m_j^2 + {\rm i}\Gamma_j)} \times \frac{1}{((p+l)^2 - M_p^2 + {\rm i}\xi)(\tilde{q}^2 - m_i^2 + {\rm i}\Gamma_i)} \,. \tag{C.2}$$

We can now evaluate this integral by the standard Feynman parametrization technique. We define

$$\mathcal{D} = l^2 + 2l(x_2 p - x_1 k - x_3 q) + x_3(q^2 - m_i^2) - x_4 m_j^2 + {\rm i}\xi + {\rm i}(x_3\Gamma_i' + x_4\Gamma_j') \,, \tag{C.3}$$

with $\Gamma_i' = \Gamma_i - \xi$. We now define the shifted momentum $r = l + (x_2 p - x_1 k - x_3 q)$, which gives $\mathcal{D} = r^2 - \Delta'$, with

$$\Delta' = x_1^2 m_e^2 + x_2^2 M_p^2 - x_3(1 - x_1 - x_2 - x_3) q^2 - 2x_1 x_2 E M_p + x_3 m_i^2 + x_4 m_j^2 - {\rm i}\xi - {\rm i}(x_3\Gamma_i' + x_4\Gamma_j') \,.$$

With this momentum shift the numerator becomes

$$\mathcal{N}^{ij}(l) = \mathcal{N}_0 + r_\mu \mathcal{N}_1^\mu + r_\mu r_\nu \mathcal{N}_2^{\mu\nu} + r_\mu r_\nu r_\rho \mathcal{N}_3^{\mu\nu\rho} \,.$$

Hence,

$$\mathcal{I}_{\rm B}^{ij} = 6 \int_0^1 \Pi_{\alpha=1}^4 \, {\rm d}x_\alpha \, \delta\left(\sum_{\alpha=1}^{4} x_\alpha - 1 \right) \times \int \frac{{\rm d}^4 r}{(2\pi)^4} \frac{\mathcal{N}_0 + r_\mu \mathcal{N}_1^\mu + r_\mu r_\nu \mathcal{N}_2^{\mu\nu} + r_\mu r_\nu r_\rho \mathcal{N}_3^{\mu\nu\rho}}{(r^2 - \Delta')^4} \,.$$

As the denominator depends only on the magnitude of r,

$$\int \frac{{\rm d}^4 r}{(2\pi)^4} \frac{r_\mu \mathcal{N}_1^\mu}{\mathcal{D}^4} = 0 \,,$$

$$\int \frac{{\rm d}^4 r}{(2\pi)^4} \frac{r_\mu r_\nu \mathcal{N}_2^{\mu\nu}}{\mathcal{D}^4} = \int \frac{{\rm d}^4 r}{(2\pi)^4} \frac{\frac{1}{4} g_{\mu\nu} \mathcal{N}_2^{\mu\nu} r^2}{\mathcal{D}^4} \,,$$

$$\int \frac{\mathrm{d}^4 r}{(2\pi)^4} \frac{r_\mu r_\nu r_\rho \mathcal{N}_3^{\mu\nu\rho}}{\mathcal{D}^4} = 0\,.$$

Let $\mathcal{N}_2$ be the shorthand notation for $\frac{1}{4} g_{\mu\nu}\mathcal{N}_2^{\mu\nu}$. Then

$$\begin{aligned}
\mathcal{I}_{\mathrm{B}}^{ij} &= 6\int_0^1 \Pi_{\alpha=1}^4 \mathrm{d}x_\alpha \delta\left(\sum_{\alpha=1}^4 x_\alpha - 1\right) \\
&\quad \times \int \frac{\mathrm{d}^4 r}{(2\pi)^4} \frac{\mathcal{N}_0 + r^2 \mathcal{N}_2}{(r^2 - \Delta')^4} \\
&= \frac{\mathrm{i}}{16\pi^2}(\mathcal{I}_0 - 2\mathcal{I}_2)\,, \\
\mathcal{I}_0 &= \int_0^1 \mathrm{d}x_3 \int_0^{1-x_3} \mathrm{d}x_2 \int_0^{1-x_3-x_2} \mathrm{d}x_1 \frac{\mathcal{N}_0}{\Delta^2}\,, \\
\mathcal{I}_2 &= \int_0^1 \mathrm{d}x_3 \int_0^{1-x_3} \mathrm{d}x_2 \int_0^{1-x_3-x_2} \mathrm{d}x_1 \frac{\mathcal{N}_2}{\Delta}\,.
\end{aligned}$$

Here

$$\begin{aligned}
\Delta &= x_1^2 m_e^2 + x_2^2 M_p^2 - x_3(1-x_1-x_2-x_3)q^2 \\
&\quad - 2x_1 x_2 E M_p + x_3 m_i^2 + (1-x_1-x_2-x_3)m_j^2 \\
&\quad - \mathrm{i}\xi - \mathrm{i}(x_3 \Gamma_i' + (1-x_1-x_2-x_3)\Gamma_j')\,.
\end{aligned}$$

If we neglect the mass of electron, then

$$\begin{aligned}
\Delta &\approx x_2^2 M_p^2 - x_3(1-x_1-x_2-x_3)q^2 - 2x_1 x_2 E M_p \\
&\quad + x_3 m_i^2 + (1-x_1-x_2-x_3)m_j^2 - \mathrm{i}\xi \\
&\quad - \mathrm{i}(x_3\Gamma_i' + (1-x_1-x_2-x_3)\Gamma_j') \\
&\equiv X x_1 + Y\,,
\end{aligned}$$

where

$$\begin{aligned}
X &= -2x_2 E M_p + x_3 q^2 - m_j^2 + \mathrm{i}\Gamma_j' \\
Y &= x_2^2 M_p^2 - x_3(1-x_2-x_3)q^2 \\
&\quad + x_3\left(m_i^2 - m_j^2\right) + (1-x_2)m_j^2 \\
&\quad - \mathrm{i}\xi - \mathrm{i}x_3(\Gamma_i' - \Gamma_j') - \mathrm{i}(1-x_2)\Gamma_j'\,.
\end{aligned}$$

$\mathcal{N}_0$ and $\mathcal{N}_2$ can be written as

$$\begin{aligned}
\mathcal{N}_0 &= Z_3 + Z_4 x_1 + Z_5 x_1^2\,, \\
\mathcal{N}_2 &= Z_1 + Z_2 x_1\,.
\end{aligned}$$

Then

$$\begin{aligned}
\mathcal{I}_0 &= \int [\mathrm{d}x] \frac{Z_3 + Z_4 x_1 + Z_5 x_1^2}{(X x_1 + Y)^2}\,, \\
\mathcal{I}_2 &= \int [\mathrm{d}x] \frac{Z_1 + Z_2 x_1}{(X x_1 + Y)}\,,
\end{aligned}$$

where

$$\int [\mathrm{d}x] \equiv \int_0^1 \mathrm{d}x_3 \int_0^{1-x_3} \mathrm{d}x_2 \int_0^{1-x_3-x_2} \mathrm{d}x_1\,.$$

The x_1 integration can be done analytically to obtain

$$\begin{aligned}
\mathcal{I}_{\mathrm{B}}^{ij} &= \frac{\mathrm{i}}{16\pi^2} \int_0^1 \mathrm{d}x_3 \int_0^{1-x_3} \mathrm{d}x_2 \\
&\quad \times \left[\frac{-2Z_1 X^2 + X(2Z_2 Y + Z_4) - 2Z_5 Y}{X^3} \ln\left(\frac{XL+Y}{Y}\right)\right. \\
&\quad + \frac{L}{X^2 Y(XL+Y)} \left\{2Z_5 Y^2 + X^2(Z_3 - 2Z_2 LY)\right. \\
&\quad \left.\left. - XY(2Z_2 Y + Z_4 - Z_5 L)\right\}\right]\,, \qquad \text{(C.4)}
\end{aligned}$$

where $L = 1 - x_3 - x_2$. The Z_i are obtained using FORM [36] and the I_{B}^{ij} are numerically computed using the Gauss–Legendre integration technique [37].

References

1. M.N. Rosenbluth, Phys. Rev. **79**, 615 (1950)
2. R.C. Walker et al., Phys. Rev. D **49**, 5671 (1994)
3. L. Andivahis et al., Phys. Rev. D **50**, 5491 (1994)
4. I.A. Qattan et al., Phys. Rev. Lett. **94**, 142 301 (2005) [nucl-ex/0410010]
5. A.I. Akhiezer, L.N. Rosentsweig, I.M. Shmushkevich, Sov. Phys. JETP **6**, 588 (1958)
6. J. Scofield, Phys. Rev. **113**, 1599 (1959)
7. J. Scofield, Phys. Rev. **141**, 1352 (1966)
8. N. Dombey, Rev. Mod. Phys. **41**, 236 (1969)
9. A.I. Akhiezer, M.P. Rekalo, Sov. J. Part. Nucl. **4**, 277 (1974)
10. R.G. Arnold, C.E. Carlson, F. Gross, Phys. Rev. C **23**, 363 (1981)
11. M.K. Jones et al., Phys. Rev. Lett. **84**, 1398 (2000)
12. O. Gayou et al., Phys. Rev. Lett. **88**, 092 301 (2002)
13. V. Punjabi et al., Phys. Rev. C **71**, 055 202 (2005)
14. V. Punjabi et al., Phys. Rev. C **71**, 069 902(E) (2005)
15. J. Arrington, C.D. Roberts, J.M. Zanotti, nucl-th/0611050
16. C.F. Perdrisat, V. Punjabi, M. Vanderhaeghen, hep-ph/0612014
17. R. Ent et al., Phys. Rev. C **64**, 054 610 (2001)
18. Y.S. Tsai, Phys. Rev. **122**, 1898 (1961)
19. L.M. Mo, Y.S. Tsai, Rev. Mod. Phys. **41**, 205 (1969)
20. L.C. Maximon, J.A. Tjon, Phys. Rev. C **62**, 054 320 (2000) [nucl-th/0002058]
21. P.A.M. Guichon, M. Vanderhaeghen, Phys. Rev. Lett. **91**, 142 303 (2003)
22. J. Arrington, Phys. Rev. C **71**, 015 202 (2005) [hep-ph/0408261]
23. P.G. Blunden, W. Melnitchouk, J.A. Tjon, Phys. Rev. Lett. **91**, 142 304 (2003) [nucl-th/0306076]
24. P.G. Blunden, W. Melnitchouk, J.A. Tjon, Phys. Rev. C **72**, 034 612 (2005) [nucl-th/0506039]
25. A.V. Afanasev, S.J. Brodsky, C.E. Carlson, Y.-C. Chen, M. Vanderhaeghen, Phys. Rev. D **72**, 013 008 (2005) [hep-ph/0502013]
26. M.P. Rekalo, E. Tomasi-Gustafsson, Eur. Phys. J. A **22**, 331 (2004)
27. M.A. Belushkin, H.W. Hammer, U.G. Meissner, hep-ph/0705.3385
28. I.A. Qattan, nucl-ex/0610006
29. G. Kleppe, R.P. Woodard, Nucl. Phys. B **388**, 81 (1992)
30. J.D. Bjorken, S.D. Drell, Relativistic Quantum Fields II (McGraw Hill Book Company, New York, 1965)
31. J.W. Moffat, Phys. Rev. D **41**, 1177 (1990)

32. R. Baldini et al, Eur. Phys. J. C **11**, 709 (1999)
33. P. Mergell, U.G. Meissner, D. Drechsel, Nucl. Phys. A **596**, 367 (1996)
34. M.A. Belushkin, H.W. Hammer, U.G. Meissner, Phys. Rev. C **75**, 035 202 (2007)
35. R. Baldini et al, Nucl. Phys. A **755**, 286 (2005)
36. J.A.M. Vermaseren, math-ph/0010025
37. W.H. Press, S.A. Teukolsky, W.T. Vetterling, B.P. Flannery, Numerical Recipes in C 2nd edn. (Cambridge University Press, Cambridge, 1992)